Modeling broadband poroelastic propagation using an asymptotic approach

D. W. Vasco
Lawrence Berkeley National Laboratory, University of California, Berkeley, CA 94720

SUMMARY

An asymptotic method, valid in the presence of smoothly-varying heterogeneity, is used to derive a semi-analytic solution to the equations for fluid and solid displacements in a poroelastic medium. The solution is defined along trajectories through the porous medium model, in the manner of ray theory. The lowest order expression in the asymptotic expansion provides an eikonal equation for the phase. There are three modes of propagation, two modes of longitudinal displacement and a single mode of transverse displacement. The two longitudinal modes define the Biot fast and slow waves which have very different propagation characteristics. In the limit of low frequency, the Biot slow wave propagates as a diffusive disturbance, in essence a transient pressure pulse. Conversely, at low frequencies the Biot fast wave and the transverse mode are modified elastic waves. At intermediate frequencies the wave characteristics of the longitudinal modes are mixed. A comparison of the asymptotic solution with analytic and numerical solutions shows reasonably good agreement for both homogeneous and heterogeneous Earth models.

Key words: poroelasticity, asymptotic methods, tomography

1 INTRODUCTION

Due to advances in subsurface monitoring, there is an increased recognition of the importance of coupled fluid flow and deformation within the Earth. For example, recent studies highlight the role of pressure changes and associated deformation in observed time-lapse seismic anomalies below, within, and above a producing reservoir (Guilbot & Smith, 2002; Landro & Stammeijer, 2004; Hatchell & Bourne, 2005; Hawkins et al., 2007; Hodgson et al., 2007; Rickett et al., 2007; Roste et al., 2007; Schutjens et al., 2007; Staples et al., 2007; Tura et al., 2005). These studies document both changes in layer position and thickness as well as seismic velocity changes due to stress variations. Such observations support conventional geodetic measurements of overburden deformation due to injection and production (Castle et al., 1969; Colazas & Strehle, 1994) as well as newer satellite-based data (Stancliffe & van der Kooij, 2001; Fielding et al., 1998) and also downhole tiltmeter data (Du et al., 2005; Maxwell et al., 2008). Furthermore, deformation of the overburden has been used to infer pressure changes and flow properties within producing reservoirs. For example, Vasco and Ferretti (2005) and Vasco et al. (2008) used satellite-based Interferometric Synthetic Aperture Radar (InSAR) measurements to image pressure changes, and ultimately permeability variations. Using a similar technique Hodgeson et al. (2007) used time-lapse 3D seismic data to image pressure changes in a deep-water reservoir in the Gulf of Mexico.

The growing emphasis on geophysical monitoring and the continuing development of time-lapse seismic and geodetic technology create a need for efficient techniques for modeling coupled fluid flow and deformation. At present, the literature on coupled modeling of fluid flow and geomechanics is vast but lacking in some respects. One difficulty follows from the complexity of modeling fully general coupled deformation and flow. Simply modeling fluid flow is a significant undertaking with a large number of processes to consider, such as multi-phase flow, chemical transport, and pressure-dependent flow properties (Bear, 1972; Peaceman, 1977; de Marsily, 1986; Wu & Pruess, 2000). And the modeling of deformation can involve elastic deformation, plastic flow, faulting and fracturing, as well as pressure and stress dependent moduli (Coussy, 2004; Showalter & Stefanelli, 2004; Jaeger et al., 2007). In this paper I will narrow the focus to coupled elastic deformation and single phase flow. Furthermore, the elastic moduli will be assumed to be time invariant. Even with these restrictions, the problem is a difficult one (Wang, 2000; Showalter, 2000), and there is a need for general, yet efficient, methods for poroelastic modeling.

Typically, there has been a trade-off between generality and efficiency in the modeling of coupled poroelastic processes. Much of the prior analytic work on both quasi-static and dynamic poroelastic modeling has been concerned with homogeneous media (Rice & Cleary, 1976; Segall, 1985; Rudnicki, 1986; Booker & Carter, 1986; Booker & Carter, 1987; Lo et al., 2006; Pride, 2005). The next level of complexity involves analytic models for poroelastic modeling in layered (Wang & Kumpel, 2003) and one-

dimensional (Simon et al., 1984; Gajo & Mongiovi, 1995) media. Though the resulting one-dimensional solutions are complete, they involve special functions and/or numerical integration and are thus difficult to interpret. The majority of work on full three-dimensional heterogeneous media is based upon purely numerical techniques, such as finite elements, finite difference, and boundary-elements (Noorishad et al., 1984; Chang et al., 1991; Lewis & Sukirman, 1993; Lewis & Ghafouri, 1997; Gutierrez & Lewis, 2002; Rutqvist et al., 2002; Minkoff et al., 2003; Minkoff et al., 2004; Masson et al., 2006; Dean et al., 2006), which, while general, do not scale well with problem size and do not provide great insight into the nature of poroelastic propagation. Furthermore, the significantly different velocities, and hence time-scales, associated with diffusive and elastic propagation, makes it difficult to model the coupled processes accurately and efficiently using numerical methods.

This paper occupies the middle-ground between the analytic and the numerical work of previous studies. Here I develop a semi-analytic solution which is valid in a medium with smoothly-varying heterogeneity of arbitrarily large magnitude. The approach, based upon an asymptotic solution to the equations governing deformation and flow in a poroelastic medium, is related to ray-based techniques for modeling wave propagation (Friedlander & Keller, 1955; Kline & Kay, 1979; Jeffrey & Kawahara, 1982; Kravtsov & Orlov, 1990; Anile et al., 1993; Bouche et al., 1997; Korsunsky, 1997; Chapman, 2004; Vasco, 2007). The asymptotic expansion follows from the application of the method of multiple scales and is appropriate for modeling propagation in a medium with regions of smoothly-varying properties separated by sharp boundaries (Jeffrey & Taniuti, 1964; Anile et al., 1993). The technique differs from a straight-forward expansion in powers of frequency (Friedlander & Keller, 1955; Keller & Lewis, 1995; Chapman, 2004) and from an expansion in the scale parameter of the poroelastic convolution operator (Hanyga & Seredyńska, 1999a; Hanyga & Seredyńska, 1999a). One advantage of this methodology is its ability to model propagation over a broad range of frequencies and to represent behavior from diffusive to hyperbolic propagation (Vasco, 2007). Furthermore, this technique is very general and applicable to the modeling of non-linear behavior (Anile et al., 1993; Jeffrey & Kawahara, 1982), such as that due to multiphase flow (Vasco, 2004) and pressure-dependent moduli (Vasco, 2009).

2 METHODOLOGY

2.1 The Governing Equations

I begin with the equations governing the evolution of the displacement fields of the solid grains $\mathbf{u}_s$ and a fluid $\mathbf{u}_f$ which are functions of the spatial coordinates $\mathbf{x}$ and time t that follow from Biot's fundamental work (Biot, 1956; Biot, 1962). These equations are the consequence of a long history of work on deformation in a fluid saturated solid (de Boer, 2000). There is some advantage in considering alternative coordinates: the solid grain displacement $\mathbf{u} = \mathbf{u}_s$ and the differential fluid displacement $\mathbf{w} = \mathbf{u}_f - \mathbf{u}_s$. Using these variables one can write the Biot equations for a fluid-saturated porous medium as

$$\nabla \cdot \tau - \nabla p_c = \rho \frac{\partial^2 \mathbf{u}}{\partial t^2} + \rho_f \frac{\partial^2 \mathbf{w}}{\partial t^2} \tag{1}$$

$$-\nabla p_f = \rho_f \frac{\partial^2 \mathbf{u}}{\partial t^2} + \eta \frac{\partial}{\partial t} \left(\frac{\mathbf{w}}{k} \right) \tag{2}$$

where τ is the deviatoric stress tensor, related to the displacement of the solid grains by the equation (Pride, 2005)

$$\tau = G \left(\nabla \mathbf{u} + \nabla \mathbf{u}^T - \frac{2}{3} \nabla \cdot \mathbf{u} \mathbf{I} \right) \tag{3}$$

where G is the shear modulus of the porous framework and $\mathbf{I}$ is the identity matrix with ones along the diagonal and zeros elsewhere. In the expression for the deviatoric stress tensor (3) I have employed the dyadic notation in which $\nabla \mathbf{u}$ is given by the outer product of the two vectors

$$\nabla \mathbf{u} = \begin{pmatrix} \frac{\partial}{\partial x}\mathbf{i} \\ \frac{\partial}{\partial y}\mathbf{j} \\ \frac{\partial}{\partial z}\mathbf{k} \end{pmatrix} \begin{pmatrix} u_x \mathbf{i} & u_y \mathbf{j} & u_z \mathbf{k} \end{pmatrix}$$

which can be thought of as a matrix (Spiegel, 1959) and $(\nabla \mathbf{u})^T$ is the transpose of this matrix. The density of the solid matrix and the pore fluid are given by ρ and ρ_f, respectively, while the fluid viscosity and permeability are denoted by η and $k(\mathbf{x})$. The average total pressure, the 'confining pressure', $p_c(\mathbf{x}, t)$, is given by the sum of the divergence of the solid displacements and the fluid displacements

$$p_c = -\left(K_u \nabla \cdot \mathbf{u} + C \nabla \cdot \mathbf{w} \right), \tag{4}$$

similarly for the fluid pressure, p_f,

$$p_f = -\left(C \nabla \cdot \mathbf{u} + M \nabla \cdot \mathbf{w} \right), \tag{5}$$

where $K_u(\mathbf{x})$ is the undrained bulk modulus, $C(\mathbf{x})$ and $M(\mathbf{x})$ are spatially-varying moduli defined by Biot (1962). The modulus M is known as the fluid-storage coefficient (Pride 2005) and represents the amount of fluid which can assimulate in a sample at constant volume. It is the poroelastic modulus most directly involved in fluid pressure diffusion. The modulus C is associated with the coupling between the fluid pressure and the elastic deformation of the solid matrix, referred to as Biot's coupling modulus.

There are numerous ways of expressing the various moduli characterizing a poroelastic medium (Wang, 2000). I shall merely quote Pride's (2005) expressions for K_u, C, and M in terms of the medium porosity ϕ, the drained bulk modulus K_d, the bulk modulus of the solid grains composing the porous medium K_s, and the bulk modulus of the fluid K_f,

$$K_u = \frac{K_d + [1 - (1-\phi)K_d/K_s]K_f/\phi}{1 + \Delta}, \tag{6}$$

$$C = \frac{(1 - K_d/K_s)K_f}{(1+\Delta)\phi}, \tag{7}$$

and

$$M = \frac{K_f}{(1+\Delta)\phi} \tag{8}$$

where Δ is a dimensionless parameter

$$\Delta = \frac{1-\phi}{\phi} \frac{K_f}{K_s} \left(1 - \frac{K_d}{(1-\phi)K_s} \right) \tag{9}$$

which is always small. The above relationships follow from the work of Biot and Willis (Biot & Willis, 1957) and Gassmann (Gassmann, 1951), and are thus known as the "Biot-Gassmann" relations (Pride 2005). The relationships (6), (7), (8), and (9) enable one to express the parameters K_u, C, and M in terms of more commonly measured quantities. Note that the parameter C, which couples the fluid pressure and the elastic displacements [equation (5)], vanishes when the drained bulk modulus K_d equals the bulk modulus of the solid grains K_s.

There is another useful way to express the moduli in terms of two other parameters, Skempton's coeff cient B and the Biot-Willis constant α. The Biot-Willis constant is related to the ratio of the compressibility of the mineral grains to the compressibility of the rock sample and is always of order 1 (Zimmerman, 2000). Skemptons coeff cient is approximately the ratio of the compressibility of the pores to the compressibility of the pore f uid and generally lies between 0 and 1. One can express both C and M in terms of K_u, B, and α,

$$C = BK_u \tag{10}$$

and

$$M = \frac{BK_u}{\alpha}. \tag{11}$$

The product αB is a poroelastic coupling parameter which indicates if one may neglect geomechanical effects when computing f uid pressure (Zimmerman, 2000)

$$\alpha B = 1 - \frac{K_d}{K_u}. \tag{12}$$

If αB is small one may generally neglect the coupling between the deformation of the solid matrix when modeling f uid pressure propagation (Zimmerman, 2000).

In equation (2) I have assumed that the permeability, $k(\mathbf{x})$ is only a function of spatial position, independent of time. In more general formulations k also varies with time and the term on the right-hand-side of equation (2) is actual a convolution between $1/k$ and $\mathbf{w}$ (Hanyga & Seredyńska, 1999a; Hanyga & Seredyńska, 1999b; Pride, 2005). The approach outlined here will work for such a general formulation, though the low frequency approximation given later must be modif ed to account for the frequency behavior of K. This more general formulation is easier to represent by transforming the governing equations into the frequency domain by taking the Fourier or Laplace transform (Bracewell, 1978) of equations (1) and (2),

$$\nabla \cdot \mathbf{T} - \nabla P_c + \omega^2 \rho \mathbf{U} + \omega^2 \rho_f \mathbf{W} = 0 \tag{13}$$

$$-\nabla P_f + \omega^2 \rho_f \mathbf{U} + i\omega \frac{\eta}{K} \mathbf{W} = 0 \tag{14}$$

where the capitial letters denote the Fourier transforms of the respective quantities and K may now be a function of the frequency ω. Thus, $\mathbf{U}(\mathbf{x}, \omega)$ is the Fourier transform of $\mathbf{u}(\mathbf{x}, t)$, a function of frequency, and similarly for $\mathbf{W}(\mathbf{x}, \omega)$, $\mathbf{T}(\mathbf{x}, \omega)$, $P_c(\mathbf{x}, \omega)$, $P_f(\mathbf{x}, \omega)$, and $K(\mathbf{x}, \omega)$. Applying the Fourier transform to equations (3), (4), and (5) I can write the governing equations (13) and (14) solely in terms of $\mathbf{U}$ and $\mathbf{W}$

$$\nabla \cdot \left[G \left(\nabla \mathbf{U} + \nabla \mathbf{U}^T - \frac{2}{3} \nabla \cdot \mathbf{U} \mathbf{I} \right) \right] \tag{15}$$

$$+ \nabla \left(K_u \nabla \cdot \mathbf{U} + C \nabla \cdot \mathbf{W} \right) + \omega^2 \rho \mathbf{U} + \omega^2 \rho_f \mathbf{W} = 0$$

$$\nabla \left(C \nabla \cdot \mathbf{U} + M \nabla \cdot \mathbf{W} \right) + \omega^2 \rho_f \mathbf{U} + i\omega \frac{\eta}{K} \mathbf{W} = 0. \tag{16}$$

2.2 An Asymptotic Solution for Deformation and Flow

Due to the presence of spatially-varying coeff cients in equations (15) and (16) it is not possible to derive an analytic solution. However, using an asymptotic approach I can derive a semi-analytic solution which is valid in the presence of smoothly-varying heterogeneity of arbitrarily large magnitude. The approach, known as the method of multiple scales, relies on a separation of scales (Anile et al., 1993; Kevorkian & Cole, 1996). In this case I assume that the heterogeneity varies at a scale-length, denoted by L, which is much larger than the scale-length over which the solid displacement and f uid pressure jump from their initial or background values to the new values after a poroelastic disturbance passes, denoted by l. Thus, $l \ll L$ and the ratio $\varepsilon = l/L$ is much smaller than 1. In the method of multiple scales one considers the problem on a spatial scale comparable to ε, transforming the problem to new spatial variables $\mathbf{X}$, where

$$\mathbf{X} = \varepsilon \mathbf{x} \tag{17}$$

are referred to as the 'slow' coordinates' Also, the solutions to equations (15) and (16) are represented as power series in ε

$$\mathbf{U}(\mathbf{X}, \omega, \theta) = e^{i\theta} \sum_{l=0}^{\infty} \varepsilon^l \mathbf{U}_l(\mathbf{X}, \omega) \tag{18}$$

$$\mathbf{W}(\mathbf{X}, \omega, \theta) = e^{i\theta} \sum_{l=0}^{\infty} \varepsilon^l \mathbf{W}_l(\mathbf{X}, \omega) \tag{19}$$

where $\theta(\mathbf{x}, \omega)$ is a function, referred to as the phase, related to the kinematics of the propagating disturbance. Because ε is small, less then 1, only the f rst few terms of these power series are signif cant. The series (18) and (19) are in the form of generalized plane wave expansions of $\mathbf{U}(\mathbf{X}, \omega, \theta)$ and $\mathbf{W}(\mathbf{X}, \omega, \theta)$, similar to that used in modeling electromagnetic and elastic waves (Luneburg, 1966; Kline & Kay, 1979; Aki & Richards, 1980; Kravtsov & Orlov, 1990). The variable $\theta(\mathbf{X}, \omega)$ is known as the phase and is associated with the travel time of the disturbance.

I consider $\mathbf{U}$ and $\mathbf{W}$ to be functions of the slow coordinates $\mathbf{X}$ and as a consequence the derivatives contained in the differential operators need to be written in terms of $\mathbf{X}$ and not in terms of $\mathbf{x}$. Using the chain rule, the derivatives may be re-written as

$$\frac{\partial \mathbf{U}}{\partial x_i} = \frac{\partial X_i}{\partial x_i} \frac{\partial \mathbf{U}}{\partial X_i} + \frac{\partial \theta}{\partial x_i} \frac{\partial \mathbf{U}}{\partial \theta} \tag{20}$$

and hence, making use of equation (17),

$$\frac{\partial \mathbf{U}}{\partial x_i} = \varepsilon \frac{\partial \mathbf{U}}{\partial X_i} + \frac{\partial \theta}{\partial x_i} \frac{\partial \mathbf{U}}{\partial \theta}. \tag{21}$$

Thus, the differential operators, which are def ned in terms of the partial derivatives with respect to the spatial coordinates, are likewise re-written as

$$\nabla \mathbf{U} = \varepsilon \nabla_{\mathbf{X}} \mathbf{U} + \nabla \theta \frac{\partial \mathbf{U}}{\partial \theta} \tag{22}$$

$$\nabla \cdot \mathbf{U} = \varepsilon \nabla_{\mathbf{X}} \cdot \mathbf{U} + \nabla \theta \cdot \frac{\partial \mathbf{U}}{\partial \theta} \tag{23}$$

where $\nabla_{\mathbf{X}}$ denotes the gradient with respect to the components of the slow variable $\mathbf{X}$.

The asymptotic solution of equations (15) and (16) is obtained by writing the differential operators in terms of $\mathbf{X}$ and θ and substituting the power series (18) and (19) for $\mathbf{U}$ and $\mathbf{W}$, respectively. The two equations that result contain inf nite sequences of terms, each containing ε to a particular power. Because ε is assumed to be small, only the terms of lowest order in ε are retained. In the next two sub-sections, I shall consider expressions containing terms of order $\varepsilon^0 \sim 1$ and ε^1. In the discussion that follows I shall suppress the subscripts on the gradient operators, that is I shall write ∇ in place of $\nabla_{\mathbf{X}}$ in order to streamline the equations. It should be understood that all operators applied to $\mathbf{U}$ and $\mathbf{W}$ are with respect to the slow coordinates $\mathbf{X}$.

2.2.1 Terms of Order $\varepsilon^0 \sim 1$: An Expression for the Phase

The full complement of terms up to order ε is given in Appendix A, equations (A8) and (A12). If I only consider terms or order $\varepsilon^0 \sim 1$, I obtain

$$G\nabla\theta\cdot\nabla\theta\frac{\partial^2\mathbf{U}_0}{\partial\theta^2}+G\nabla\theta\nabla\theta\cdot\frac{\partial^2\mathbf{U}_0}{\partial\theta^2}-\frac{2}{3}G\nabla\theta\cdot\left(\nabla\theta\cdot\frac{\partial^2\mathbf{U}_0}{\partial\theta^2}\right)$$

$$+K_u\nabla\theta\nabla\theta\cdot\frac{\partial^2\mathbf{U}_0}{\partial\theta^2}+\omega^2\rho\mathbf{U}_0+C\nabla\theta\nabla\theta\cdot\frac{\partial^2\mathbf{W}_0}{\partial\theta^2}+\omega^2\rho_f\mathbf{W}_0=0 \tag{24}$$

and

$$C\nabla\theta\nabla\theta\cdot\frac{\partial^2\mathbf{U}_0}{\partial\theta^2}+\omega^2\rho_f\mathbf{U}_0+M\nabla\theta\nabla\theta\cdot\frac{\partial^2\mathbf{W}_0}{\partial\theta^2}+\omega^2\tilde{\rho}\mathbf{W}_0=0 \tag{25}$$

where

$$\tilde{\rho}=\frac{i\eta}{\omega K}. \tag{26}$$

In these equations I have substituted in the power series expansions (18) and (19). Due to the specif c form of the dependence of $\mathbf{U}_0$ and $\mathbf{W}_0$ on the phase, the derivatives with respect to θ are given by

$$\frac{\partial\mathbf{U}_0}{\partial\theta}=i\mathbf{U}_0 \tag{27}$$

$$\frac{\partial\mathbf{W}_0}{\partial\theta}=i\mathbf{W}_0 \tag{28}$$

and similarly for higher-order derivatives. Also, let the vector $\mathbf{p}$ denote the gradient of θ

$$\mathbf{p}=\nabla\theta, \tag{29}$$

the gradient vector of the phase function. Substituting for the derivatives with respect to θ and for $\nabla\theta$ in equations (24) and (25), I obtain equations for $\mathbf{U}_0$ and $\mathbf{W}_0$

$$\beta\mathbf{pp}\cdot\mathbf{U}_0-\alpha\mathbf{U}_0+C\mathbf{pp}\cdot\mathbf{W}_0-\omega^2\rho_f\mathbf{W}_0=0 \tag{30}$$

and

$$C\mathbf{pp}\cdot\mathbf{U}_0-\omega^2\rho_f\mathbf{U}_0+M\mathbf{pp}\cdot\mathbf{W}_0-\omega^2\tilde{\rho}\mathbf{W}_0=0 \tag{31}$$

where

$$\beta=K_u+\frac{1}{3}G \tag{32}$$

and

$$\alpha=\omega^2\rho-Gp^2 \tag{33}$$

[See Appendix A, equations (A14) and (A15)]. I can write equations (30) and (31) in matrix form

$$\begin{pmatrix}\alpha\mathbf{I}-\beta\mathbf{pp}\cdot\mathbf{I} & \omega^2\rho_f\mathbf{I}-C\mathbf{pp}\cdot\mathbf{I}\\ \omega^2\rho_f\mathbf{I}-C\mathbf{pp}\cdot\mathbf{I} & \omega^2\tilde{\rho}\mathbf{I}-M\mathbf{pp}\cdot\mathbf{I}\end{pmatrix}\begin{pmatrix}\mathbf{U}_0\\ \mathbf{W}_0\end{pmatrix}=\begin{pmatrix}\mathbf{0}\\ \mathbf{0}\end{pmatrix}. \tag{34}$$

From linear algebra it is known that the system of equations (34) has a non-trivial solution if and only if the determinant of the coeff - cient matrix vanishes (Noble & Daniel, 1977). The vanishing of the determinant def nes a polynomial equation in the components of the vector $\mathbf{p}$ with coeff cients which are functions of the medium parameters. From the def nition of $\mathbf{p}$, equation (29), one f nds that the vanishing of the determinant also def nes a non-linear partial differential equation for $\theta(\mathbf{X},\omega)$, the eikonal equation associated with propagation in a poroelastic medium (Kravtsov & Orlov, 1990). While it is possible to form the polynomial equation directly from the determinant of the coeff cient matrix of equation (34), I follow a less direct route, avoiding some rather tedious algebra.

The approach I take works with the eigenvalues and eigenvectors associated with the coeff cient matrix in equation (34). There is a connection between the eigenvalues of the coeff cient matrix and the determinant of the coeff cient matrix. Specif cally, the product of the eigenvalues, an invariant of the coeff cient matrix, equals the determinant (Noble & Daniel, 1977). In this approach, I f rst observe that the vectors

$$\mathbf{e}=\begin{pmatrix}y_1\mathbf{p}\\ y_2\mathbf{p}\end{pmatrix}, \tag{35}$$

and

$$\mathbf{e}^{\perp}=\begin{pmatrix}y_1\mathbf{p}^{\perp}\\ y_2\mathbf{p}^{\perp}\end{pmatrix}, \tag{36}$$

where y_1 and y_2 are scalar coeff cients and $\mathbf{p}^{\perp}$ denotes a vector perpendicular to $\mathbf{p}$, look like candidate eigenvectors of the system of equations (34). That is, vectors which satisfy the equation

$$\mathbf{\Gamma e}=\lambda\mathbf{e} \tag{37}$$

where $\mathbf{\Gamma}$ is the coeff cient matrix in (34) and λ is a scalar to be determined. A similar equation holds for for $\mathbf{e}^{\perp}$ with a different scalar, which I will denote by $\lambda^{\perp}$. From equation (29) one observes that the vector $\mathbf{p}$ is perpendicular to the phase front, the iso-surface of constant phase while $\mathbf{p}^{\perp}$ lies within the plane tangent to the iso-surface. These vectors denote longitudinal and transverse modes of propagation and, as I shall show, propagate with differing velocities. As such, I consider each mode separately, f rst examining deformation in the direction of $\mathbf{p}$, the longitudinal displacement vector.

Longitudinal Displacements

If I substitute the vector $\mathbf{e}$, def ned in (35) into the eigenvalue equation (37), where the matrix $\mathbf{\Gamma}$ is given by the matrix in (34), I f nd that

$$\left[(\alpha-\beta p^2)y_1+(\omega^2\rho_f-Cp^2)y_2\right]\mathbf{p}=\lambda y_1\mathbf{p} \tag{38}$$

$$\left[(\omega^2\rho_f-Cp^2)y_1+(\omega^2\tilde{\rho}-Mp^2)y_2\right]\mathbf{p}=\lambda y_2\mathbf{p}, \tag{39}$$

where $p^2=\mathbf{p}\cdot\mathbf{p}$ is the square of the magnitude of the vector $\mathbf{p}$. I may write equations (38) and (39) as a single matrix equation

$$\begin{pmatrix}\alpha-\beta p^2-\lambda & \omega^2\rho_f-Cp^2\\ \omega^2\rho_f-Cp^2 & \omega^2\tilde{\rho}-Mp^2-\lambda\end{pmatrix}\begin{pmatrix}y_1\\ y_2\end{pmatrix}=\begin{pmatrix}0\\ 0\end{pmatrix} \tag{40}$$

for y_1 and y_2. As noted above, this equation has a non-trivial solution if and only if the determinant of the coeff cient matrix vanishes. This is a polynomial equation containing the medium parameters, p, and λ. Now, the medium parameters are assumed to be f xed but p and λ may both be considered as unknowns in the polynomial. Thus, there is some freedom in specifying the values of λ and p. I take advantage of this f exibility and set λ equal to zero in order to simplify the expression for the determinant and obtain an equation solely in terms of p

$$\det\begin{pmatrix}\alpha-\beta p^2 & \omega^2\rho_f-Cp^2\\ \omega^2\rho_f-Cp^2 & \omega^2\tilde{\rho}-Mp^2\end{pmatrix} \tag{41}$$

$$=(\alpha-\beta p^2)(\omega^2\tilde{\rho}-Mp^2)-(\omega^2\rho_f-Cp^2)^2=0.$$

Equation (41) is a quadratic equation for p^2

$$(p^2)^2 - \frac{\omega^2(\rho M + \tilde{\rho} H - 2\rho_f C)}{(HM - C^2)} p^2 + \frac{\omega^4(\rho\tilde{\rho} - {\rho_f}^2)}{(HM - C^2)} = 0 \tag{42}$$

where H is given by

$$H = K_u + \frac{4}{3}G. \tag{43}$$

The quadratic equation (42) has the solution

$$p^2 = \frac{\omega^2}{2}\left[\gamma \pm \sqrt{\gamma^2 - \frac{4(\rho\tilde{\rho} - {\rho_f}^2)}{HM - C^2}}\right] \tag{44}$$

where γ is the auxiliary parameter given by

$$\gamma = \frac{\rho M + \tilde{\rho} H - 2\rho_f C}{HM - C^2}. \tag{45}$$

This expression for the squared 'slowness' is similar to that given by Pride (2005) for a plane wave in a homogeneous medium. However, equation (44) is valid for a medium with smoothly varying heterogeneity of arbitrary magnitude. Factoring γ out from under the radical I can write equation (44) as

$$p^2 = \frac{\gamma\omega^2}{2}\left[1 \pm \sqrt{1 - \frac{4}{\gamma^2}\frac{(\rho\tilde{\rho} - {\rho_f}^2)}{HM - C^2}}\right] \tag{46}$$

or

$$p^2 = \frac{\gamma\omega^2}{2}\left[1 \pm \sqrt{1 - \zeta}\right] \tag{47}$$

where

$$\zeta = \frac{4(\rho\tilde{\rho} - {\rho_f}^2)(HM - C^2)}{(\tilde{\rho} H + \rho M - 2\rho_f C)^2}. \tag{48}$$

Expression (46) for the slowness provides a means for tracing rays and calculating the propagation path for a transient disturbance (Aki & Richards, 1980; Kravtsov & Orlov, 1990). Making use of the def nition of $\mathbf{p}$ I can write equation (47) as a differential equation for $\theta(\mathbf{x}, \omega)$

$$\nabla\theta \cdot \nabla\theta = \frac{\gamma\omega^2}{2}\left[1 \pm \sqrt{1 - \zeta}\right], \tag{49}$$

an eikonal equation for the longitudinal mode of displacement in a poroelastic medium. This scalar partial differential equation is equivalent to a system of ordinary differential equations for a trajectory $\mathbf{X}(r)$ and the vector $\mathbf{p}(r)$ (Courant & Hilbert, 1962)

$$\frac{d\mathbf{X}}{dr} = \frac{\mathbf{p}}{\chi} \tag{50}$$

$$\frac{d\mathbf{p}}{dr} = \nabla\chi \tag{51}$$

where $\chi(\mathbf{X}, \omega)$ is the slowness, def ned as

$$\chi(\mathbf{X}, \omega) = \omega\sqrt{\frac{\gamma}{2}\left[1 \pm \sqrt{1 - \zeta}\right]} \tag{52}$$

and r is the distance along the trajectory $\mathbf{X}(r)$. One can integrate the system of equations using a numerical technique such as a shooting method coupled to a globally convergent Newton-Raphson algorithm (Press et al., 1992). In addition, one may derive an integral expression for the phase $\theta(r, \omega)$ by writing the eikonal equation (49) in ray coordinates, taking the square root, and integrating

$$\theta(r, \omega) = \int_{\mathbf{X}(r)} \chi(\mathbf{X}(r')dr' \tag{53}$$

or, more compactly,

$$\theta(r, \omega) = \omega\tau(r) \tag{54}$$

where

$$\tau(r) = \int_{\mathbf{X}(r)} \sqrt{\frac{\gamma}{2}\left[1 \pm \sqrt{1 - \zeta}\right]}dr'. \tag{55}$$

The coupled differential equations (50) and (51) are used to construct trajectories or rays between a source and an observation point. The trajectories form the basis for eff cient forward modeling of poroelastic propagation. Furthermore, they allow for semi-analytic expressions for model parameter sensitivities and the solution of the inverse problem (Menke, 1984). For example, the rays form the basis for travel time tomographic imaging which has proven highly successful in seismology (Nolet, 1987; Iyer & Hirahara, 1993) among other f elds. Note that, in the most general setting the slowness can be complex and one must resort to complex ray tracing (Kravtsov et al., 1999; Amodei et al., 2006). Complex eikonals appear when the propagation behavior can vary from hyperbolic wave propagation to diffusive decay, as in broadband electromagnetic modeling (Vasco, 2007).

An alternative to ray tracing involves solving the eikonal equation, the non-linear partial differential equation (49), numerically. This approach is now well established and has been applied to a number of practical problems and seems quite stable (Sethian, 1999). It was introduced to seismology by Vidale (1988) and has been generalized in various ways. Note that, to date, the method has not yet been extended to complex eikonal equations. Thus, currently, it can only be applied to certain regimes of poroelastic propagation.

Transverse Displacements

Following a similar procedure, I consider the potential eigenvector $\mathbf{e}^{\perp}$, given by equation (36), and the resulting equation

$$\mathbf{\Gamma}\mathbf{e}^{\perp} = \lambda^{\perp}\mathbf{e}^{\perp} \tag{56}$$

where $\mathbf{\Gamma}$ is the coeff cient matrix in (34) and $\lambda^{\perp}$ is a scalar to be determined. Taking into account the coeff cient matrix (34) and carrying out the matrix-vector multiplications by $\mathbf{p}^{\perp}$ I arrive at the following linear system of equations

$$\left[\alpha y_1 + \omega^2\rho_f y_2\right]\mathbf{p}^{\perp} = \lambda^{\perp} y_1 \mathbf{p}^{\perp} \tag{57}$$

$$\left[\omega^2\rho_f y_1 + \omega^2\tilde{\rho} y_2\right]\mathbf{p}^{\perp} = \lambda^{\perp} y_2 \mathbf{p}^{\perp}, \tag{58}$$

which may be written as a matrix equation for y_1 and y_2,

$$\begin{pmatrix} \alpha - \lambda^{\perp} & \omega^2\rho_f \\ \omega^2\rho_f & \omega^2\tilde{\rho} - \lambda^{\perp} \end{pmatrix}\begin{pmatrix} y_1 \\ y_2 \end{pmatrix} = \begin{pmatrix} 0 \\ 0 \end{pmatrix}. \tag{59}$$

The linear system of equations has a non-trivial solution if

$$\det\begin{pmatrix} \alpha - \lambda^{\perp} & \omega^2\rho_f \\ \omega^2\rho_f & \omega^2\tilde{\rho} - \lambda^{\perp} \end{pmatrix} = 0 \tag{60}$$

which, after noting that $\alpha = \omega^2\rho - Gp^2$, and setting $\lambda^{\perp}$ equal to zero, produces a quadratic equation for p

$$\omega^2\tilde{\rho}\left(\omega^2\rho - Gp^2\right) = \left(\omega^2\rho_f\right)^2. \tag{61}$$

Thus, I have produced an equation for p

$$p^2 = \omega^2 \frac{\left[\rho - \left(\frac{\rho_f}{\tilde{\rho}}\right)\rho_f\right]}{G} \tag{62}$$

which leads to the eikonal equation for transverse displacements in a poroelastic medium

$$\nabla\theta \cdot \nabla\theta = \omega^2 \frac{\left[\rho - \left(\frac{\rho_f}{\tilde{\rho}}\right)\rho_f\right]}{G}, \tag{63}$$

a simple modif cation of the eikonal equation for an elastic medium

$$\nabla\theta \cdot \nabla\theta = \omega^2 \frac{\rho}{G} \tag{64}$$

(Aki & Richards, 1980). As for the longitudinal displacements, I can def ne a slowness, $\chi(\mathbf{X}, \omega)$ for the transverse motion,

$$\chi(\mathbf{X}, \omega) = \omega \sqrt{\frac{\left[\rho - \left(\frac{\rho_f}{\tilde{\rho}}\right)\rho_f\right]}{G}}. \tag{65}$$

As expected, the transverse displacement depends upon the moduli ρ and G. In addition, the transverse displacement also depends upon the properties of the f uid and the permeability through the presence of ρ_f and $\tilde{\rho}$ in (62).

Note that, while the longitudinal component is uniquely determined as the normal to the surface of constant phase, via its def nition (29), the transverse component can lie within the two-dimensional plane tangent to this surface. Thus, there is some degree of freedom for the transverse component to change orientation. Partitioning the transverse mode of propagation into components leads to the study of the vertical and horizontal shear waves.

2.2.2 Terms of Order ε: An Expression for the Amplitude

Next, I consider terms of order ε, which gives two sets of equations containing phase and amplitude terms. My starting point is the set of equations (A16) and (A17) in Appendix A. As noted in the previous sub-section, there are two modes of propagation: longitudinal motion and transverse motion, each with a distinct propagation speed. To make progress I need to consider the longitudinal and transverse modes of propagation in greater detail.

Longitudinal Displacements

For longitudinal displacements $\mathbf{U}$ is a vector in the same direction as $\mathbf{p}$. For simplicity, I assume that all the contributions in the series (18) and (19) are proportional to $\mathbf{p}$. Further, assume that $\mathbf{U}_1$ and $\mathbf{W}_1$ are vectors which satisfy equation (34). Thus, the terms containing U_1 and W_1 cancel and I obtain two sets of equations for U_0 and W_0, given that the phase θ is found by solving the eikonal equation (49),

$$2\mathbf{p}\left(\mathbf{p}\cdot\nabla G\right)U_0 - \frac{2}{3}\nabla G p^2 U_0 + \nabla K_u p^2 U_0 + \nabla C p^2 W_0 \tag{66}$$

$$+G\left[\left(\nabla\cdot\mathbf{p}\right)\mathbf{p}U_0 + 2\mathbf{p}\cdot\nabla\left(\mathbf{p}U_0\right)\right]$$

$$+G\left[\nabla\cdot(\mathbf{p}U_0)\mathbf{p} + U_0\mathbf{p}\cdot\nabla\mathbf{p} + \mathbf{p}\cdot\{\nabla(\mathbf{p}U_0)\}^T\right]$$

$$-\frac{2}{3}G\left[\nabla\left(p^2U_0\right) + \mathbf{p}\nabla\cdot\left(\mathbf{p}U_0\right)\right]$$

$$+K_u\left[\nabla\left(p^2U_0\right) + \mathbf{p}\nabla\cdot\left(\mathbf{p}U_0\right)\right]$$

$$+C\left[\nabla\left(p^2W_0\right) + \mathbf{p}\nabla\cdot\left(\mathbf{p}W_0\right)\right] = 0$$

and

$$\nabla C p^2 U_0 + \nabla M\left(p^2 W_0\right) \tag{67}$$

$$+C\left[\nabla\left(p^2U_0\right) + \mathbf{p}\nabla\cdot\left(\mathbf{p}U_0\right)\right]$$

$$+M\left[\nabla\left(p^2W_0\right) + \mathbf{p}\nabla\cdot\left(\mathbf{p}W_0\right)\right] = 0.$$

Note that equations (66) and (67) comprise six equations for the two unknowns U_0 and W_0. The system can be reduced to two equations for two unknowns by projecting onto the vector $\hat{\mathbf{p}}$, a unit vector in the direction of the vector $\mathbf{p}$. After projecting onto $\hat{\mathbf{p}}$, expanding the dyadic and differential operators, and grouping like terms, I arrive at the equations

$$2pH\hat{\mathbf{p}}\cdot\nabla U_0 + \left(H\nabla\cdot\mathbf{p} + 2H\hat{\mathbf{p}}\cdot\nabla p + p\hat{\mathbf{p}}\cdot\nabla H\right)U_0$$

$$+2pC\hat{\mathbf{p}}\cdot\nabla W_0 + \left(C\nabla\cdot\mathbf{p} + 2C\hat{\mathbf{p}}\cdot\nabla p + p\hat{\mathbf{p}}\cdot\nabla C\right)W_0 = 0 \tag{68}$$

and

$$2pC\hat{\mathbf{p}}\cdot\nabla U_0 + \left(C\nabla\cdot\mathbf{p} + 2C\hat{\mathbf{p}}\cdot\nabla p + p\hat{\mathbf{p}}\cdot\nabla C\right)U_0$$

$$+2pM\hat{\mathbf{p}}\cdot\nabla W_0 + \left(M\nabla\cdot\mathbf{p} + 2M\hat{\mathbf{p}}\cdot\nabla p + p\hat{\mathbf{p}}\cdot\nabla M\right)W_0 \tag{69}$$

where, as def ned in (43), $H = K_u + 4/3G$. Because the gradients of U_0 and W_0 are projected onto the trajectory $\mathbf{X}(r)$ in equations (68) and (69), they represent the changes along the ray path. Thus, I may consider equations (68) and (69) to be a system of differential equations for U_0 and W_0 and write all projected gradients as derivatives with respect to r the position along the trajectory $\mathbf{X}(r)$. Also, because of the eikonal equation (47) or (49), I can replace p by the slowness $\chi(\mathbf{X}, \omega)$, as def ned in equation (52). I can write these equations more compactly if I def ne the coeff cients

$$\Upsilon_{11} = 2\chi H, \tag{70}$$

$$\Omega_{11} = H\left[\nabla\cdot\mathbf{p} + 2\frac{d\chi}{dr} + \chi\frac{d(\ln H)}{dr}\right], \tag{71}$$

$$\Upsilon_{12} = 2\chi C, \tag{72}$$

$$\Omega_{12} = C\left[\nabla\cdot\mathbf{p} + 2\frac{d\chi}{dr} + \chi\frac{d(\ln C)}{dr}\right], \tag{73}$$

$$\Upsilon_{21} = 2\chi C, \tag{74}$$

$$\Omega_{21} = C\left[\nabla\cdot\mathbf{p} + 2\frac{d\chi}{dr} + \chi\frac{d(\ln C)}{dr}\right], \tag{75}$$

$$\Upsilon_{22} = 2\chi M, \tag{76}$$

and

$$\Omega_{22} = M\left[\nabla\cdot\mathbf{p} + 2\frac{d\chi}{dr} + \chi\frac{d(\ln M)}{dr}\right]. \tag{77}$$

Then, equations (68) and (69) can be written as

$$\boldsymbol{\Upsilon}\frac{d\mathbf{V}}{dr} + \boldsymbol{\Omega}\mathbf{V} = 0 \tag{78}$$

where

$$\mathbf{V} = \begin{pmatrix} U_0 \\ W_0 \end{pmatrix} \tag{79}$$

and $\boldsymbol{\Upsilon}$ and $\boldsymbol{\Omega}$ are matrices with the coeff cients given above. Note, both the matrices $\boldsymbol{\Upsilon}$ and $\boldsymbol{\Omega}$ are symmetric and the matrix $\boldsymbol{\Upsilon}$

$$\boldsymbol{\Upsilon} = 2\chi\begin{pmatrix} H & C \\ C & M \end{pmatrix} \tag{80}$$

has the explicit inverse

$$\boldsymbol{\Upsilon}^{-1} = \frac{1}{2\chi(HM - C^2)} \begin{pmatrix} M & -C \\ -C & H \end{pmatrix} \tag{81}$$

which is def ned as long as χ and $HM - C^2$ do not vanish. Multiplying the terms of equation (78) by $\boldsymbol{\Upsilon}^{-1}$ results in the equation

$$\frac{d\mathbf{V}}{dr} = -\boldsymbol{\Gamma}\mathbf{V} \tag{82}$$

where

$$\boldsymbol{\Gamma} = \boldsymbol{\Upsilon}^{-1}\boldsymbol{\Omega}. \tag{83}$$

Note that for a homogeneous medium

$$\boldsymbol{\Gamma} = \boldsymbol{\Upsilon}^{-1}\boldsymbol{\Omega} = \frac{\nabla \cdot \mathbf{p}}{2\chi}\boldsymbol{\Upsilon}^{-1}\boldsymbol{\Upsilon} = \frac{\nabla \cdot \mathbf{p}}{2\chi}\mathbf{I} \tag{84}$$

and equation (82) decouples to produce two equations which may be solved exactly for U_0 and W_0

$$U_0(\mathbf{X}) = {A_U}^0 \exp\left[-\int_{\mathbf{X}(r)} \frac{\nabla \cdot \mathbf{p}}{2\chi} dr\right] \tag{85}$$

$$W_0(\mathbf{X}) = {A_W}^0 \exp\left[-\int_{\mathbf{X}(r)} \frac{\nabla \cdot \mathbf{p}}{2\chi} dr\right] \tag{86}$$

where ${A_U}^0$ and ${A_W}^0$ are the initial amplitudes of the solid and relative f uid displacements and $\mathbf{X}(r)$ denotes the trajectory which provides the path of integration. This is simply the amplitude decay due to the geometrical spreading of the wavef eld as it propagates away from the source (Kline & Kay, 1979; Kravtsov & Orlov, 1990).

For a heterogeneous medium the f rst-order system of equations (82) can be solved in its present form using a numerical technique or, as shown in Appendix B, the system can be written as two uncoupled, second-order differential equations for U_0 and W_0. The governing equation for the amplitude of the solid displacement vector is given by

$$\frac{d^2U_0}{dr^2} + \Psi_1\frac{dU_0}{dr} + \Psi_2 U_0 = 0, \tag{87}$$

a linear, second-order differential equation for U_0 with variable coeff cients given in terms of the elements of the matrix $\boldsymbol{\Gamma}$:

$$\Psi_1(r) = \Gamma_{12}\frac{d}{dr}\left(\frac{1}{\Gamma_{12}}\right) + \Gamma_{11} + \Gamma_{22} \tag{88}$$

$$\Psi_2(r) = \Gamma_{12}\frac{d}{dr}\left(\frac{\Gamma_{11}}{\Gamma_{12}}\right) - \Gamma_{12}\Gamma_{21} + \Gamma_{11}\Gamma_{22} \tag{89}$$

Similarly, I can derive a governing equation for W_0

$$\frac{d^2W_0}{dr^2} + \Phi_1\frac{dW_0}{dr} + \Phi_2 W_0 = 0, \tag{90}$$

where

$$\Phi_1(r) = \Gamma_{21}\frac{d}{dr}\left(\frac{1}{\Gamma_{21}}\right) + \Gamma_{11} + \Gamma_{22} \tag{91}$$

$$\Phi_2(r) = \Gamma_{21}\frac{d}{dr}\left(\frac{\Gamma_{22}}{\Gamma_{21}}\right) - \Gamma_{12}\Gamma_{21} + \Gamma_{11}\Gamma_{22}. \tag{92}$$

Such decoupling in the frequency domain was noted by (Berryman, 1983). These two scalar, ordinary differential equations may be solved eff ciently using widely available numerical techniques (Press et al., 1992). Alternatively, an asymptotic technique may be used to derive semi-analytic solutions (Keller & Lewis, 1995).

Transverse Displacements

For transverse displacements $\mathbf{U}$ is a vector lying in the plane perpendicular to $\mathbf{p}$, which I shall denote by $\mathbf{p}^\perp$. As noted earlier, there is some freedom in the orientation of $\mathbf{p}^\perp$ as it may lie within a two-dimensional plane. Under the same assumptions invoked for the longitudinal displacements, I consider the terms of order ε^1, as given in equations (A16) and (A17) for the case in which $\mathbf{U}_0$, $\mathbf{U}_1$, $\mathbf{W}_0$ and $\mathbf{W}_1$ are oriented in the direction $\mathbf{p}^\perp$. The resulting equations are

$$\begin{aligned} &\mathbf{p}(\nabla G \cdot \mathbf{p}^\perp)U_0 + \mathbf{p}^\perp(\nabla G \cdot \mathbf{p})U_0 \\ &+G\left[\mathbf{p}^\perp(\nabla \cdot \mathbf{p})U_0 + 2\mathbf{p} \cdot \nabla(U_0\mathbf{p}^\perp)\right] \\ &+G\left[\mathbf{p}\nabla \cdot (U_0\mathbf{p}^\perp) + (\mathbf{p}^\perp \cdot \nabla\mathbf{p})U_0 + \mathbf{p} \cdot \nabla(U_0\mathbf{p}^\perp)^T\right] \end{aligned} \tag{93}$$

$$-\frac{2}{3}G\mathbf{p}\nabla \cdot (U_0\mathbf{p}^\perp) + K_u\mathbf{p}\nabla \cdot (U_0\mathbf{p}^\perp) + C\mathbf{p}\nabla \cdot (W_0\mathbf{p}^\perp) = 0$$

and

$$C\mathbf{p}\nabla \cdot \left(U_0\mathbf{p}^\perp\right) + M\mathbf{p}\nabla \cdot \left(W_0\mathbf{p}^\perp\right) = 0. \tag{94}$$

Equations (93) and (94) represent six equations for the two unknowns U_0 and W_0. I can reduce the number of equations by projecting the displacement vectors onto a unit vector in the direction of motion $\hat{\mathbf{p}}^\perp$. In doing so, the terms containing W_0 in equation (93) and all the terms in equation (94) vanish, resulting in a single equation for the amplitude function U_0.

$$\begin{aligned} &p^3(\hat{\mathbf{p}} \cdot \nabla G)U_0 + G\left[p^2(\nabla \cdot \mathbf{p})U_0 + 2\mathbf{p}^\perp \cdot \mathbf{p} \cdot \nabla\left(U_0\mathbf{p}^\perp\right)\right] \\ &+G\left[\mathbf{p}^\perp \cdot \mathbf{p}^\perp \cdot \nabla\mathbf{p}U_0 + \mathbf{p}^\perp \cdot \mathbf{p} \cdot \nabla(U_0\mathbf{p}^\perp)\right] = 0. \end{aligned} \tag{95}$$

Thus, the transverse solid displacement is completely uncoupled from the f uid displacement vector $\mathbf{W}$. Expanding the dyadic expressions and combining terms produces a scalar equation for U_0

$$3Gp\hat{\mathbf{p}} \cdot \nabla U_0 + p\hat{\mathbf{p}} \cdot \nabla G U_0 + G\left[\nabla \cdot \mathbf{p} + 2\hat{\mathbf{p}} \cdot \nabla(p^2)\right]U_0 = 0. \tag{96}$$

Noting again that the projection of the gradient operator onto the unit vector $\hat{\mathbf{p}}$ signif es the rate of change of the quantity with respect to distance r along the trajectory $\mathbf{X}$, I can write equation (96) as

$$3Gp\frac{dU_0}{dr} + G\left[\nabla \cdot \mathbf{p} + 2\frac{dp}{dr} + p\frac{d(\ln G)}{dr}\right]U_0 = 0. \tag{97}$$

Noting that the eikonal equation allows one to write the magnitude of the vector $\mathbf{p}$ in terms of the slowness $\chi(\mathbf{X}, \omega)$ [see equation (65)] and def ning

$$\Pi = 3\chi G \tag{98}$$

and

$$\Sigma = G\left[\nabla \cdot \mathbf{p} + 2\frac{d\chi}{dr} + \chi\frac{d(\ln G)}{dr}\right], \tag{99}$$

I can write equation (97) as a f rst-order ordinary differential equation for U_0

$$\Pi\frac{dU_0}{dr} + \Sigma U_0 = 0 \tag{100}$$

which may be written

$$\frac{dU_0}{dr} = -\frac{\Sigma}{\Pi}U_0. \tag{101}$$

Equation (101) has the explicit solution

$$U_0(\mathbf{X}) = {A_U}^0 \mathrm{e}^{-\varsigma(\mathbf{X})} \tag{102}$$

where

$$\varsigma(\mathbf{X}) = \int_{\mathbf{X}(r)} \frac{\Sigma}{\Pi} dr \tag{103}$$

and ${A_U}^0$ is the initial displacement amplitude. Thus, it is possible to derive an analytic expression for the amplitude of the transverse displacement. From the coeff cients (98) and (99) it is clear the the transverse displacement only depends upon the shear modulus G, the slowness χ, and the geometrical spreading of the trajectories as measured by $\nabla \cdot \mathbf{p}$.

2.3 The Nature of the Longitudinal Biot Slow and Fast Waves in the Limit of Low Frequency

It is diff cult to make def nitive statements regarding the nature of the two solutions in equation (47) due to the coupling of the f uid f ow and the elastic deformation in the matrix. However, if I consider a low-frequency solution it is possible to make further progress. I should point out that in considering lower frequencies the scale length of the disturbance will lengthen. Hence, I am limiting the solution to a medium with heterogeneity of a suff ciently long scale length. At lower frequencies the Biot equations decouple, as noted by Pride (2005) and Lo et al. (2006), and the numerator and denominator of ζ are dominated by $\tilde{\rho}$ [see equation (48)]. As indicated by the def nition (26), if K is not a function of frequency then $\tilde{\rho}$ is proportional to $1/\omega$, becoming large as ω approaches zero. Thus, as ω approaches zero ζ approaches

$$\zeta = -i \frac{4\rho(HM - C^2)K}{\eta H^2} \omega.$$

When K is a function of frequency ω, the behavior of ζ depends upon the relationship of K to the frequency. For low frequencies, ζ smaller than 1, I can use the binomial expansion to write the square root term in equation (47) as a power series in ζ. Retaining only the f rst two terms of the expansion I obtain

$$p^2 = \frac{\gamma\omega^2}{2} \left[1 \pm (1 - \frac{1}{2}\zeta) \right]. \tag{104}$$

The magnitude of the phase gradient vector $\mathbf{p}$ is related to the inverse of the velocity of the propagating disturbance (Aki & Richards, 1980), so that larger values of p correspond to slower moving features. Because ζ is taken to be smaller than 1 the f rst root

$$p^2 = \frac{\gamma\omega^2}{2} \left[2 - \frac{1}{2}\zeta \right] \tag{105}$$

is known as the 'Biot slow wave', corresponding to a propagating, diffusive wave, related to a f uid pressure transient (Vasco et al., 2000; Vasco, 2008a). The second root results in an expression for the 'Biot fast wave'

$$p^2 = \frac{\gamma\zeta\omega^2}{4} \tag{106}$$

which is the porous medium equivalent of an elastic wave and propagates with much less attenuation and a much higher velocity (Pride, 2005). Accounting for the exact expressions for γ, equation (45), and ζ, equation (48), I can write the equation (106) for the fast wave as

$$p^2 = \omega^2 \frac{\rho\tilde{\rho} - {\rho_f}^2}{\tilde{\rho}H + \rho M - 2\rho_f C} \tag{107}$$

or as

$$p^2 = \omega^2 \frac{\rho - \frac{\rho_f}{\tilde{\rho}}\rho_f}{H + \frac{\rho}{\tilde{\rho}}M - 2\frac{\rho_f}{\tilde{\rho}}C}. \tag{108}$$

Comparing the expression for a porous medium (108) to that for a purely elastic medium

$$p^2 = \omega^2 \frac{\rho}{H}, \tag{109}$$

the modif cations required to account for poroelastic processes are apparent. Note that, while the frequency dependence of an elastic disturbance (109) is straight-forward and represents hyperbolic wave propagation, the frequency dependence of a disturbance in a poroelastic medium (108) is rather more complicated due to the presence of the parameter $\tilde{\rho}$, which is def ned in (26). This is particularly true if K is also a function of frequency, leading to more complex propagation, including dispersion and dissipation. In the next two sub-sections I consider these two modes of longitudinal displacement in somewhat more detail. Specif cally, I derive the form of the zeroth-order asymptotic solutions $\mathbf{U}_0$ and $\mathbf{W}_0$ in both the frequency and time domains in the limit of low frequency. As noted by (Pride, 2005), the boundary of the low frequency regime lies in the kilo-Hertz to mega-Hertz range and covers the vast majority of seismic and hydrologic f eld experiments.

2.3.1 The Biot Slow Wave

First, consider the Biot slow wave whose slowness is given by equation (105), which may written as

$$p^2 = \gamma\omega^2 - \frac{\gamma\zeta\omega^2}{4} \tag{110}$$

in the low frequency limit. In the limit as ω approaches zero I f nd that

$$\lim_{\omega \to 0} \gamma = \frac{\tilde{\rho}H}{HM - C^2} = \frac{i\eta}{\omega K} \frac{H}{(HM - C^2)} \tag{111}$$

and

$$\lim_{\omega \to 0} \zeta = 4\rho \frac{\omega K}{i\eta} \frac{(HM - C^2)}{H^2} \tag{112}$$

and equation (110) takes the form

$$p^2 = \frac{i\omega\eta}{K} \frac{H}{(HM - C^2)} - 4\frac{\rho\omega^2}{H} \tag{113}$$

which, for ω near zero, is dominated by the f rst term on the right

$$p^2 = \frac{i\omega\eta}{K} \frac{H}{(HM - C^2)}. \tag{114}$$

Drawing upon equation (114) I can write the low frequency approximation to the eikonal equation for the Biot slow wave as

$$\nabla\theta \cdot \nabla\theta = \frac{i\omega\eta}{K} \frac{H}{(HM - C^2)}. \tag{115}$$

As stated previously in the discussion associated with equations (49) through (55), I can def ne the slowness as the square root of the right-hand-side of equation (115),

$$\chi(\mathbf{X}, \omega) = \sqrt{\frac{i\omega\eta}{K} \frac{H}{(HM - C^2)}}. \tag{116}$$

Expressing the eikonal equation in ray coordinates, along the trajectory $\mathbf{X}(r)$ I arrive at an integral expression for the phase $\theta(r, \omega)$

$$\theta(r, \omega) = \int_{\mathbf{X}(r)} \chi(\mathbf{X}(r')) dr' \tag{117}$$

or, moving $i\omega$ outside the integral and defining

$$\tau(r) = \int_{\mathbf{X}(r)} \sqrt{\frac{\eta}{K}\frac{H}{(HM - C^2)}}dr', \tag{118}$$

the phase may be written in the form

$$\theta(r,\omega) = \sqrt{i\omega}\tau(r). \tag{119}$$

Now consider the zeroth-order term in the power series representation of $\mathbf{U}(\mathbf{X},\omega,\theta)$ and $\mathbf{W}(\mathbf{X},\omega,\theta)$ [equations (18) and (19)]

$$\mathbf{U}(\mathbf{X},\omega,\theta) = e^{i\theta}\mathbf{U}_0(\mathbf{X},\omega) \tag{120}$$

$$\mathbf{W}(\mathbf{X},\omega,\theta) = e^{i\theta}\mathbf{W}_0(\mathbf{X},\omega) \tag{121}$$

which provides a suitable approximation to the solid and fluid displacements if ε is small. Substituting the expression for the phase, $\theta(r,\omega)$, and the fact that $\mathbf{U}_0 = U_0\mathbf{p}$ and $\mathbf{W}_0 = W_0\mathbf{p}$ the above expressions take the form

$$\mathbf{U}(\mathbf{X},\omega,\theta) = e^{\sqrt{-i\omega}\tau(\mathbf{X})}U_0(\mathbf{X},\omega)\mathbf{p} \tag{122}$$

$$\mathbf{W}(\mathbf{X},\omega,\theta) = e^{\sqrt{-i\omega}\tau(\mathbf{X})}W_0(\mathbf{X},\omega)\mathbf{p} \tag{123}$$

where $\mathbf{X}(r)$ a point on the trajectory a distance r from the source of the disturbance. Inverse Fourier transforming equations (122) and (123) back into the time domain, using the fact that the inverse Fourier transform of a product is the convolution of the inverse Fourier transforms and the inverse transform of $e^{\sqrt{-i\omega}}$ is a Gaussian (Spiegel, 1990; Virieux et al., 1994)

$$\mathbf{u}(\mathbf{X},t,\theta) = \frac{\tau}{2\sqrt{\pi t^3}}e^{-\tau^2/4t}H(t) * u_0(\mathbf{X},t)\mathbf{p} \tag{124}$$

$$\mathbf{w}(\mathbf{X},t,\theta) = \frac{\tau}{2\sqrt{\pi t^3}}e^{-\tau^2/4t}H(t) * w_0(\mathbf{X},t)\mathbf{p} \tag{125}$$

where $*$ signifies a temporal convolution and $u_0(\mathbf{X},t)$, $w_0(\mathbf{X},t)$ are the inverse transforms of $U_0(\mathbf{X},\omega)$ and $W_0(\mathbf{X},\omega)$, and $H(t)$ is the Heaviside or step-function which jumps in value from zero to one at $t = 0$.

The phase behavior in (124) and (125) contains a Gaussian impulse response which is the solution to the diffusion equation (Carslaw & Jaeger, 1959). This form of the solution agrees with previous studies in homogeneous media where it was found that the low frequency Biot slow wave satisfies a diffusion-type equation [see (Pride, 2005) and (Lo et al., 2006)]. Such a solution is also in agreement with solutions for quasi-static pressure and displacement in a poroelastic medium (Rudnicki, 1986; Wang & Kumpel, 2003; Vasco, 2008a). The solutions (124) and (125) decay rapidly with propagation distance and do not behave like elastic waves. However, it is still possible to consider the propagating transient disturbance as a type of wave and to define an 'arrival time' and to use such arrival times to perform something akin to travel time tomography (Virieux et al., 1994; Vasco et al., 2000; Shapiro et al., 2002; Vasco et al., 2008). In order to gain some insight, consider the solution in the time domain, equation (124), when the amplitude function $u_0(\mathbf{X},t)$ does not depend upon time. The peak of the displacement occurs when the temporal derivative vanishes, that is when

$$\frac{\partial\mathbf{u}(\mathbf{X},t,\theta)}{\partial t} = \frac{\tau}{2\sqrt{\pi}}e^{-\tau^2/4t}\left[-\frac{3}{2\sqrt{t^5}} + \frac{\tau^2}{4\sqrt{t^7}}\right]u_0(\mathbf{X})\mathbf{p} \tag{126}$$

is equal to zero. This condition is satisfied when the quantity inside the square brackets vanishes, that is when

$$t = \frac{\tau^2}{6} \tag{127}$$

or

$$\tau = \sqrt{6T_{peak}} \tag{128}$$

where T_{peak} is the time at which the displacement attains a maximum value. Thus the 'phase', $\tau(\mathbf{X})$ is proportional to the square root of the time at which the peak deformation occurs. One can use this quantity to define an 'arrival time' for the diffusive transient displacement (Virieux et al., 1994). For more a complicated source-time function $u_0(\mathbf{X},t)$ it is necessary to remove it from the recorded displacement before computing the arrival time. If the source-time function is known, it may be removed by deconvolution in the time or frequency domain (Bracewell, 1978).

The expressions for the matrix and fluid displacements (124) and (125) correspond to a delta function source in time. That is, to an impulsive source in which the displacement is non-zero at a single point in time. Due to the diffusive nature of the propagation of the Biot slow wave such an initial pulse will not propagate very far from the source. Rather, it is more common to have a step function source in which fluid is introduced at a point for a long period of time. That is, initially the flow rate is zero and then steps up to some non-zero value very quickly and is maintained at that rate for a long period of time. In that way the constant flux of mass or energy propagates some distance from the source. I can obtain this type of source by integrating the delta function in time. The integral of a delta function is a step function (Bracewell, 1978), and the integral of the impulse response is given by

$$\mathbf{u}(\mathbf{X},t,\theta) = \int_0^t \frac{\tau}{2\sqrt{\pi y^3}}e^{-\tau^2/4y}dy * u_0(\mathbf{X},t)\mathbf{p} \tag{129}$$

$$\mathbf{w}(\mathbf{X},t,\theta) = \int_0^t \frac{\tau}{2\sqrt{\pi y^3}}e^{-\tau^2/4y}dy * w_0(\mathbf{X},t)\mathbf{p}. \tag{130}$$

The integral is related to the complementary error function (Press et al., 1992) and so I can write equations (129) and (130) as

$$\mathbf{u}(\mathbf{X},t,\theta) = \operatorname{erfc}\left(\frac{\tau}{2\sqrt{t}}\right) * u_0(\mathbf{X},t)\mathbf{p} \tag{131}$$

$$\mathbf{w}(\mathbf{X},t,\theta) = \operatorname{erfc}\left(\frac{\tau}{2\sqrt{t}}\right) * w_0(\mathbf{X},t)\mathbf{p} \tag{132}$$

which is similar to the solution for fluid diffusion due to constant fluid injection of withdrawal (Theis, 1935).

2.3.2 The Biot Fast Wave

Now I consider the second possible value for p^2 in equation (104), associated with the minus sign, which results in

$$p^2 = \frac{\gamma\zeta\omega^2}{4} \tag{133}$$

or, considering the limits of equations (111) and (112),

$$p^2 = \omega^2\frac{\rho}{H} \tag{134}$$

which is identical to the slowness for an elastic medium [equation (109)]. The associated eikonal equation, obtained by substituting $\nabla\theta$ for $\mathbf{p}$ [see the definition of $\mathbf{p}$, equation (29)], is

$$\nabla\theta\cdot\nabla\theta = \omega^2\frac{\rho}{H}. \tag{135}$$

As was done previously for the Biot slow wave, I can define the slowness

$$\chi(\mathbf{X},\omega) = \omega\sqrt{\frac{\rho}{H}}. \tag{136}$$

Consideration of the eikonal equation in ray coordinates allows one to write the phase as the integral

$$\theta(r,\omega) = \omega \int_{\mathbf{X}(r)} \sqrt{\frac{\rho}{H}} dr', \tag{137}$$

or as

$$\theta(r,\omega) = \omega\tau(r) \tag{138}$$

where

$$\tau(r) = \int_{\mathbf{X}(r)} \sqrt{\frac{\rho}{H}} dr'. \tag{139}$$

Now consider the zeroth-order approximation to the solid and f uid displacements given by

$$\mathbf{U}(\mathbf{X},\omega,\theta) = e^{i\theta}\mathbf{U}_0(\mathbf{X},\omega) \tag{140}$$

$$\mathbf{W}(\mathbf{X},\omega,\theta) = e^{i\theta}\mathbf{W}_0(\mathbf{X},\omega). \tag{141}$$

Substituting in the expression (138) for the phase θ and accounting for the fact that $\mathbf{U}_0$ and $\mathbf{W}_0$ are longitudinal displacements (in the $\mathbf{p}$ direction), I arrive at the frequency domain representation

$$\mathbf{U}(\mathbf{X},\omega,\theta) = e^{i\omega\tau(\mathbf{X})}U_0(\mathbf{X},\omega)\mathbf{p} \tag{142}$$

$$\mathbf{W}(\mathbf{X},\omega,\theta) = e^{i\omega\tau(\mathbf{X})}W_0(\mathbf{X},\omega)\mathbf{p}. \tag{143}$$

Applying the inverse Fourier transform to equations (142) and (143) produces the time domain expressions

$$\mathbf{u}(\mathbf{X},t) = \delta(t-\tau) * u_0(\mathbf{X},t)\mathbf{p} \tag{144}$$

$$\mathbf{w}(\mathbf{X},t) = \delta(t-\tau) * w_0(\mathbf{X},t)\mathbf{p} \tag{145}$$

where $\delta(t)$ is the delta function. The convolution with the delta function may be evaluated exactly (Bracewell, 1978), resulting in

$$\mathbf{u}(\mathbf{X},t) = u_0(\mathbf{X},t-\tau)\mathbf{p} \tag{146}$$

$$\mathbf{w}(\mathbf{X},t) = w_0(\mathbf{X},t-\tau)\mathbf{p}. \tag{147}$$

Thus, the waveforms are just shifted versions of the source waveform combined with changes due to propagation described by the amplitude equations (87) and (90). This is in keeping with previous studies which indicate that the Biot fast wave is in essence an elastic wave propagating in the poroelastic medium (Pride, 2005; Lo et al., 2006).

2.4 Nature of the Transverse Displacement in the Limit of Low Frequency

The squared slowness associated with the transverse displacement is given by equation (62)

$$p^2 = \omega^2 \frac{\left[\rho - \left(\frac{\rho_f}{\phi}\right)\rho_f\right]}{G}. \tag{148}$$

In order to obtain the exact dependence on the f ow properties η and K and frequency ω, I substitute the expression for $\tilde{\rho}$, equation (26)

$$p^2 = \frac{\omega^2\rho}{G} + \frac{i\omega^3 K(\rho_f)^2}{G\eta} \tag{149}$$

which, for low frequency, is dominated by the f rst term on the right-hand-side. Thus, at low frequencies

$$p^2 = \frac{\omega^2\rho}{G} \tag{150}$$

and

$$\chi(\mathbf{X},\omega) = \omega\sqrt{\frac{\rho}{G}}. \tag{151}$$

Consideration of the eikonal equation in ray coordinates enables me to write the phase as

$$\theta(r,\omega) = \omega\tau(r) \tag{152}$$

where

$$\tau(r) = \int_{\mathbf{X}(r)} \sqrt{\frac{\rho}{G}} dr'. \tag{153}$$

The zeroth-order approximation to the solid displacement is given by

$$\mathbf{U}(\mathbf{X},\omega,\theta) = e^{i\omega\tau(\mathbf{X})}U_0(\mathbf{X},\omega)\mathbf{p}^{\perp} \tag{154}$$

Applying the inverse Fourier transform to equations (154) produces the time domain expression

$$\mathbf{u}(\mathbf{X},t) = \delta(t-\tau) * u_0(\mathbf{X},t)\mathbf{p}^{\perp} \tag{155}$$

where $\delta(t)$ is the delta function. The convolution with the delta function may be evaluated exactly (Bracewell, 1978), resulting in

$$\mathbf{u}(\mathbf{X},t) = u_0(\mathbf{X},t-\tau)\mathbf{p}^{\perp} \tag{156}$$

where τ is the time delay corresponding to the transverse displacement, equation (153).

2.5 Propagation across an Interface

As with ray theoretical approaches for modeling elastic wave propagation, one can include a discontinuous change in material properties as a boundary and subject the wavef elds to the appropriate boundary conditions (Aki & Richards, 1980; Chapman, 2004). Hence, one can use the asymptotic expressions given above in models containing layering, faults, and other structural and stratigraphic features. Due to the presence of the Biot slow wave and the f uid displacement f eld, the interaction of the wavef eld with an interface in a poroelastic medium will be a somewhat richer topic, with four possible ref ected and transmitted waves [fast longitudinal, fast in-plane transverse (SV), fast out-of-plane transverse (SH), and slow longitudinal] for each incident wave. The longitudinal mode of propagation will have two associated displacement f elds, one associated with the solid displacement $\mathbf{U}$ and the other associated with the relative f uid displacement $\mathbf{W}$. The transverse mode of propagation will only include solid displacements, as indicated by the equation governing the amplitude (95). A discussion of ref ection and transmission coeff cients warrants an entire paper, and will be the subject of future work. Such a treatment involves a direct extension of the results for an elastic medium (Aki & Richards, 1980; Chapman, 2004).

2.6 Computation of the Complete Displacement Response

Given that there are two modes of longitudinal propagation, the Biot slow and fast waves, with very different propagation characteristics, some thought must be given to the computation of the complete response at a given point. In particular, the fact that the Biot fast waves decays slowly, essentially as an elastic wave, means that a particular station may receive contributions from many different

locations. Stated another way, a large pressure change can generate a continuous contribution of Biot fast waves as it propagates (Vasco 2008a). Because the Biot fast waves can travel signif cant distances without much decay, one must account for these contributions in computing the displacement response at a given location. Conversely, a Biot fast wave can generate a Biot slow wave near the receiver and contribute to the local pressure response. This process may be responsible to the dynamic triggering of micro-seismicity by large, remote earthquakes.

In this sub-section I will touch upon the summation of Biot fast wave contributions from a pressure source, as generated by the injection or withdrawal of f uid from a well. This is a particularly common situation, encountered in groundwater, geothermal, petroleum, and waste disposal activities. I consider an impulsive pressure source, which will generate both Biot slow and fast waves. The Biot slow wave will propagate from the source point $\mathbf{X}_s$ to an intermediate location $\mathbf{X}_i$ and the disturbance is given by equation (124),

$$\mathbf{u}(\mathbf{X}_i,\mathbf{X}_s;t) = \frac{\tau(\mathbf{X}_i,\mathbf{X}_s)}{2\sqrt{\pi t^3}} \exp\left[-\tau(\mathbf{X}_i,\mathbf{X}_s)^2/4t\right] \tag{157}$$

$$\times u_0(\mathbf{X}_s,\mathbf{X}_i)\mathbf{p}_s(\mathbf{X}_i)$$

where $u_0(\mathbf{X}_i,\mathbf{X}_x)$ represents the amplitude decay of the slow wave due to propagation from $\mathbf{X}_s$ to $\mathbf{X}_i$. Similarly, $\tau(\mathbf{X}_i,\mathbf{X}_s)$ represents the accumulated phase change as the diffusive slow wave propagates from the source to $\mathbf{X}_i$. As the Biot slow wave propagates from the source location $\mathbf{X}_s$ to the intermediate point in the medium it will generate, or shed, Biot fast waves. Once the fast waves are generated, say at the point $\mathbf{X}_i$, they will propagate to the receiver point $\mathbf{X}_r$ according to equation (146). I shall denote the accumulated phase due to the propagation of the Biot fast wave from $\mathbf{X}_i$ to the receiver point $\mathbf{X}_r$ by $\tau(\mathbf{X}_r,\mathbf{X}_i)$ and similarly for the amplitude decay $u_0(\mathbf{X}_r,\mathbf{X}_i)$. One consideration in the generation of the longitudinal displacement for the Biot fast wave is that the trajectories of the outgoing fast wave may differ from that of the incoming Biot slow wave. Thus, I include a term accounting for the projection of the displacement associated with the Biot slow wave onto the displacement direction of the outgoing fast wave. The contribution to the displacement at the receiver located at $\mathbf{X}_r$ for a wave that traveled as a slow wave to from $\mathbf{X}_s$ to $\mathbf{X}_i$ and then as a fast wave from $\mathbf{X}_i$ to $\mathbf{X}_r$ is

$$\mathbf{u}(\mathbf{X}_r,\mathbf{X}_s;t) = \frac{\tau(\mathbf{X}_i,\mathbf{X}_s)}{2\sqrt{\pi\left[t-\tau(\mathbf{X}_r,\mathbf{X}_i)\right]^3}} \tag{158}$$

$$\exp\left[-\tau(\mathbf{X}_i,\mathbf{X}_s)^2/4(t-\tau(\mathbf{X}_r,\mathbf{X}_i))\right]$$

$$\times u_0(\mathbf{X}_r,\mathbf{X}_i)u_0(\mathbf{X}_i,\mathbf{X}_s)\mathbf{p}_f(\mathbf{X}_i)\cdot\mathbf{p}_s(\mathbf{X}_i)\mathbf{p}_f(\mathbf{X}_r).$$

The total displacement at $\mathbf{X}_r$, $\mathbf{u}(\mathbf{X}_r,t)$, is obtained by summing or integrating over all intermediate points $\mathbf{X}_i$

$$\mathbf{u}(\mathbf{X}_r,t) = \int_V \mathbf{u}(\mathbf{X}_r,\mathbf{X}_s;t)d\mathbf{X}_i. \tag{159}$$

One can evaluate this integral directly using numerical methods or approximate it using an asymptotic technique (Dingle, 1973). The procedure is similar to the quasi-static calculation for the solid displacement due to a pressure source presented in Wang (2000, p. 110).

3 APPLICATIONS

In this section I implement the methodology described above and use it to model f uid pressure changes and solid matrix displacements due to f uid injection into a borehole. Two particular cases are considered: homogeneous and heterogeneous media, and the results are compared with predictions from a f nite difference code and an analytic solution for a homogeneous medium. I shall only be concerned with the computation of the direct longitudinal slow and fast arrivals. That is, I will not compute conversions between slow and fast arrivals, as indicated in equations (158) and (159). An example of such a calculation, in the case of quasi-static poroelastic propagation, was given in Vasco (2008a).

3.1 Propagation in a Homogeneous Medium

Here, I am interested in modeling the evolution of f uid pressure and solid displacement in a homogeneous medium induced by a rapid pressure pulse (Figure 1). The half-width of the pulse is less than 0.1 s and the pressure source is activated at 0.2 s. The medium is a homogeneous porous whole space with a solid bulk modulus of 30.5 GPa, an undrained bulk modulus of 20.5 GPa, a f uid bulk modulus of 2.2 GPa, a shear modulus of 8.4 GPa, a solid density of 2.5 gm/cc, a f uid density of 1.0 gm/cc, a porosity of 0.1, and a hydraulic conductivity of 3.0 $\times 10^{-12}$. In order to reduce the computation I shall consider a two dimensional problem, modeling the propagation within a vertical slice of the Earth. A numerically stable f nite difference code (Masson et al., 2006) is used to calculate the pressure and displacements due to the injection. In Figure 2 three snap-shots of the pressure variation in the two-dimensional whole space are shown. Note that by 1000 s the pressure variation has reached the boundaries of the model and the predictions of the f nite difference code will be inf uenced by this interaction.

For a homogeneous medium I can use the expression given in (Wang & Kumpel, 2003) for the quasi-static pressure variation. The inertial terms are probably not signif cant in the governing equation for pressure if the frequency is low. This conjecture is verif ed through a comparison of pressure predictions made using the f nite-difference approach of (Masson et al., 2006), the analytic predictions of (Wang & Kumpel, 2003), and the asymptotic expression given by equation (125) of this paper (Figure 3). In general, the agreement between the three methods is fairly good though the agreement with the numerical results deteriorate somewhat after the peak pressure is obtained. The differences after the peak pressure may be due to the interaction of the pressure with the boundary in the numerical modeling (Figure 2). The differences between the asymptotic pressure estimates and the analytic and the f nite-difference estimates are shown in greater detail in Figure 4 where I plot the absolute error as a function of time. In general, the error is less then 2 % of the peak pressure value plotted in Figure 3.

The inertial terms cannot be neglected when calculating the elastic displacement of the solid matrix. Doing so will give the correct elastic quasi-static response to the pressure changes near the injection point, that is the response modeled using equations (158) and (159). However, the quasi-static solution does not contain the Biot fast wave which is generated by the rapid pressure change due to injection. For an analytic model of the Biot fast wave I use the expressions provided by (Gajo & Mongiovi, 1995). In addition, I generate a numerical solution using the f nite-difference code of (Masson et al., 2006). Three snap-shots, generated within the f rst 0.3 s after the start of injection, are shown in Figure 5. Note the interaction of the Biot fast wave, which is essentially an elastic wave,

with the boundaries of the mesh by 0.28 s. The boundaries generate reflections which impact the predictions made after that time. This points to some of the limitations of numerical approaches for modeling poroelastic processes. The time scale of the pressure variation (Figure 2) is significantly different from that for the elastic wave (Figure 5). Thus, the elastic wave traverses the entire numerical modeling grid by 300 iterations of the finite difference code. About 1,000,000 iterations are necessary to model the propagation of the pressure disturbance from the source to the edge of the modeling grid, taking roughly 2 hours of CPU time. If I had doubled the size of the grid to avoid spurious reflections then the amount of computation increases by four times, requiring 8 hours of CPU times.

In Figure 6 I compare the predictions of the numerical code with those of the analytic solution of (Gajo & Mongiovi, 1995) and the asymptotic solution given for the Biot fast wave, equation (146). When the phase term is real, the analytic and asymptotic solutions are shifted versions of the source function, after we account for the mapping of pressure into displacement which occurs at the source. The predictions of the three methods are fairly close until the displacement peak. Following the peak displacement, the numerical predictions deviate from the analytic and asymptotic predictions. As with the pressure, this may be due to the interaction of the finite-difference results with the boundary of the modeling grid. In addition, one must be careful when including the source-time function as noted by (Chapman, 1985). For example, for an elastic wave one must consider the analytic time series which contains both the source-time function as well as its Hilbert transform. The disagreement is shown in more detail is Figure 7, where one finds exact agreement between the analytic and asymptotic displacements and increasing discrepancies between the numerical solution and the analytic and asymptotic solutions.

3.2 Propagation in a Heterogeneous Medium

In an effort to examine propagation in a heterogeneous medium I perturbed the uniform model given above, using linear and quadratic functions to generate a two-dimensional velocity model (Figure 8). The resulting model constrains a high velocity zone bounded above and below by low velocity regions. The source is located at (0.5 km, 0.5 km), within the high velocity zone, while the receiver lies at the upper edge of the high velocity zone. From the results of the finite difference pressure calculations, one observes that the pressure propagation is very much influenced by the heterogeneities (Figure 9). The rather asymmetric pressure distribution contrasts sharply with that of the homogeneous medium (Figure 2). Solving the eikonal equation (49) numerically using the fast marching method of (Sethian, 1999), which was introduced in seismology by (Vidale, 1988) one can compute the travel time contours (Figure 10). The trajectories for asymptotic modeling can be generated by marching down the gradient of the travel time field (Sethian, 1999). Such a trajectory connecting the source and receiver is shown in Figure 10. The calculation of the phase field and the generation of the trajectory took around 5 CPU seconds on a workstation. In Figure 11 I compare the numerical solution produced by the finite-difference code with the asymptotic solution given above. Note that the analytic solution is no longer valid, due to the presence of heterogeneity. Overall, there is relatively good agreement between the two predictions. The discrepancy between the two solutions is shown in more detail in Figure 12. Generally, the two solutions lie within 2-4 percent of each other.

In Figure 13 I compare the displacement of the solid matrix associated with the Biot fast wave. As before, the solution was truncated due to interference from boundary reflections in the numerical modeling. There is general agreement between the two solutions and most of the differences occur after the peak of the pulse. As noted above, the numerical solution is influenced by the presence of the boundary in this time interval. The agreement between the asymptotic solution and the numerical predictions could be improved by expanding the modeling grid and accounting for the exact position of the source and receiver within the modeling grid. Furthermore, using the full frequency response, given in equation (49), rather than the low frequency response (146), and the analytic source function (Chapman, 1985), should improve the agreement.

4 CONCLUSIONS

An asymptotic approach provides a useful technique for modeling the propagation of a disturbance in a poroelastic medium with smoothly-varying elastic and flow properties. Because the expansion is in terms of a scale parameter defined by the ratio of the width of the disturbance to the scale-length of the heterogeneity, the solution should be valid across a range of frequencies as long as the heterogeneity is sufficiently smooth. The expressions for the phase and amplitudes of the longitudinal Biot fast and slow displacements and the transverse displacements are simple extensions of expressions for displacements in an elastic medium. In the limit of low frequency, the expressions capture the diffusive nature of the Biot slow wave and the hyperbolic wave-like nature of the longitudinal Biot fast wave and the transverse displacement. At higher frequencies the propagation can contain elements of diffusive and hyperbolic propagation and the slowness, as given in equation (47), can be complex and require complex ray tracing (Kravtsov et al., 1999; Amodei et al., 2006; Vasco, 2007). As noted above, it is possible to account for interfaces in the methodology, by treating a discontinuity as a boundary condition. An example of the refraction at a boundary for quasi-static propagation in a poroelastic medium was given in Vasco (2008).

The trajectory-based solution derived in the paper provides additional insight into the manner in which the properties of the medium influence the propagation of disturbances within a poroelastic Earth model. For example, the three modes of propagation, the fast and slow longitudinal displacements and the fast transverse displacement, are given by the three sets of eigenvalues and eigenvectors of the matrix (34). The three additional solutions required of the 6 by 6 matrix are provided by disturbances propagating in the reverse direction. The exact combination of the medium parameters and frequency contributing to the phase velocity of each mode of propagation follows from equations (47) and (62). The variation of amplitude with propagation distance for each mode of propagation is given by the transport equations (87) and (90) for the longitudinal displacements, and the expression (102) for the transverse displacement. These expressions are particularly useful when solving the inverse problem, in which observations are used to infer properties within the Earth (Iyer & Hirahara, 1993). For example, the expressions allow the inverse problem to be partitioned into a travel time inverse problem (Aki et al., 1976) and an amplitude inverse problem (Thomson, 1983). The travel time inverse problem is quasi-linear in nature and has better convergence properties to a solution than the amplitude inverse problem (Nolet, 1987). It is also possible to formulate an efficient, low-order waveform inversion algorithm based upon the asymptotic solution (Vasco et al., 2003). The asymptotic formalism used here also unifies two classes

of inverse problems: the inversion of displacement and seismic data (Vasco et al., 2003) and the inversion of fluid flow data (Vasco et al., 2000; Vasco, 2008b).

There a number of avenues by which to extend this work. First, one could generalize the governing equations such that the moduli depend on the stress field and/or the fluid pressure. Second, one could consider multi-phase fluid flow and the attendant complications. Third, more complicated rheologies, such as plasticity, could be invoked for the solid matrix. The method of multiple scales may be used for such generalizations because it is applicable to nonlinear (Jeffrey & Kawahara, 1982; Anile et al., 1993) and coupled (Korsunsky, 1997) processes. There are also a number of possible applications of the methodology including the study of deformation accompanying reservoir production mentioned in the Introduction. In addition, it would be of interest to explore the consequences of the conversion of longitudinal displacements between the Biot fast and slow waves. As noted by Pride (2005) and illustrated in Vasco (2008a), in a heterogeneous poroelastic medium, fast waves can generate slow waves and vice-versa. Given the differences in the nature of propagation of these two modes, this leads to some interesting effects, such as the rapid appearance of elastic deformation as compared to the appearance the gradual appearance of pressure change (Vasco 2008a). Such conversions may be a factor in the remote triggering of micro-earthquakes by dynamic strains generated during a major earthquake (Hill et al., 1993).

ACKNOWLEDGMENTS

This work was supported by the Assistant Secretary, Office of Basic Energy Sciences of the U. S. Department of Energy under contract DE-AC02-05CH 11231. I wish to thank S. Pride and Y. Masson for supplying the finite difference code for computing displacements in a poroelastic medium. All computations were carried out at the Center for Computational Seismology, Berkeley Laboratory.

REFERENCES

Aki, K. & Richards, P. G., 1980. *Quantitative Seismology*, Freeman and Sons.

Aki, K., Christoffersson, A., & Husebye, E. S., 1976. Determination of the three-dimensional seismic structures of the lithosphere, *J. Geophys. Res.*, **82**, 277–296.

Amodei, D., Keers, H., Vasco, D., & Johnson, L., 2006. Computation of uniform wave forms using complex rays, *Physical Review*, **73**, 036704/1–14.

Anile, A., Hunter, J. K., Pantano, P., & Russo, G., 1993. Ray methods for nonlinear waves in f uids and plasmas, *Longman Scientif c and Technical*, **40**, 104–108.

Bear, J., 1972. *Dynamics of Fluids in Porous Media*, Dover Publications.

Berryman, J. G., 1983. Dispersion of extensional waves in f uid-saturated porous cylinders at ultrasonic frequencies, *J. Acoust. Soc. Am.*, **74**, 1805–1812.

Biot, M. A., 1956. Theory of propagation of elastic waves in a f uid-saturated porous solid. i. low-frequency range, *J. Acoust. Soc. Am.*, **28**, 168–178.

Biot, M. A., 1962. Mechanics of deformation and acoustic propagation in porous media, *J. Appl. Phys.*, **33**, 1482–1498.

Biot, M. A. & Willis, D. G., 1957. The elastic coeff cients of the theory of consolidation, *J. Appl. Mech.*, **24**, 594–601.

Booker, J. R. & Carter, J. P., 1986. Analysis of a point sink embedded in a porous elastic half space, *Int. J. Numer. Anal. Meth. Geomech.*, **10**, 137–149.

Booker, J. R. & Carter, J. P., 1987. Elastic consolidation around a point sink embedded in a half-space with anisotropic permeability, *Int. J. Numer. Anal. Meth. Geomech.*, **11**, 61–77.

Bouche, D., Molinet, F., & Mittra, R., 1997. *Asymptotic Methods in Electromagnetics*, Springer-Verlag, Berlin.

Bracewell, R. N., 1978. *The Fourier Transform and Its Applications*, McGraw-Hill, New York.

Carslaw, H. S. & Jaeger, J. C., 1959. *Conduction of Heat in Solids*, Oxford University Press, Oxford.

Castle, R. O., Yerkes, R. F., & Riley, F. S., 1969. A linear relationship between liquid production and oil-related subsidence, in *Land Subsidence*, edited by L. J. Tison, pp. 597–604, Association Internationale d'Hydrologie Scientif que publication.

Chang, A. H.-D., Badmus, T., & Beskos, D. E., 1991. Integral equation for dynamic poroelasticity in frequency domain with bem solution, *J. Eng. Mech.*, **117**, 1136–1157.

Chapman, C. H., 1985. Ray theory and its extensions: Wkbj and maslov seismograms, *Journal of Geophysics*, **58**, 27–43.

Chapman, C. H., 2004. *Fundamentals of Seismic Wave Propagation*, Cambridge University Press.

Colazas, X. C. & Strehle, R. W., 1994. Subsidence in the wilmington oil f eld, long beach, california, in *Subsidence due to Fluid Withdrawal*, edited by G. V. Chilingarian, E. C. Donaldson, & T. F. Yen, Elsevier Science.

Courant, R. & Hilbert, D., 1962. *Methods of Mathematical Physics*, Interscience, New York.

Coussy, O., 2004. *Poromechanics*, John Wiley and Sons, West Sussex.

de Boer, R., 2000. *Theory of Porous Media*, Springer-Verlag, Berlin.

de Marsily, G., 1986. *Quantitative Hydrogeology*, Academic Press, San Diego.

Dean, R., Gai, X., Stone, C., & Minkoff, S., 2006. A comparison of techniques for coupling porous f ow and geomechanics, *SPE Journal*, **11**, 132–140.

Dingle, R. B., 1973. *Asymptotic Expansions: Their Derivation and Interpretation*, Academic Press, London.

Du, J., Brissenden, S. J., McGillivray, P., Bourne, S., Hofstra, P., Davis, E. J., Roadarmel, W. J., Wolhart, S. L., Marsic, S., Gusek, R., & Wright, C. A., 2005. Mapping reservoir volume changes during cyclic steam f ooding using tiltmeter-based surface deformation measurements, in *SPE International Thermal Operations and Heavy Oil Symposium*, p. 97848, CHOA.

Fielding, E. J., Blom, R. G., & Goldstein, R. M., 1998. Rapid subsidence over oil f elds measured by sar interferometry, *Geophysical Research Letters*, **25**, 3215–3218.

Friedlander, F. G. & Keller, J. B., 1955. Asymptotic expansions of solutions of $(\nabla^2 + k^2)u = 0$, *Comm. Pure Appl. Math.*, **8**, 387.

Gajo, A. & Mongiovi, L., 1995. An analytical solution for the transient response of saturated linear elastic porous media, *Intern. J. Num. Anal. Meth. Geomech.*, **19**, 399–413.

Gassmann, F., 1951. Elastic waves through a packing of spheres, *Geophysics*, **16**, 673–685.

Guilbot, J. & Smith, B., 2002. 4-d constrained depth conversion for reservoir compaction estimation: Application to ekof sk f eld, *The Leading Edge*, **21**, 302–308.

Gutierrez, M. & Lewis, R. W., 2002. Coupling of f uid f ow and deformation in underground formations, *J. Eng. Mech.*, **128**, 779–787.

Hanyga, A. & Seredyńska, M., 1999. Some effects of the memory kernel singularity on wave propagation and inversion in poroelastic media-i. forward problems, *Geophysical Journal International*, **137**, 319–335.

Hanyga, A. & Seredyńska, M., 1999. Asymptotic ray theory in poro- and viscoelastic media, *Wave Motion*, **30**, 175–195.

Hatchell, P. & Bourne, S., 2005. Rocks under strain: Strain-induced time-lapse time shifts are observed for depleting reservoirs, *The Leading Edge*, **17**, 1222–1225.

Hawkins, N., Howe, S., Hollingworth, S., Conroy, G., BenBrahim, L., Tindle, C., Taylor, N., Joffroy, G., & Onaisi, A., 2007. Production-induced stresses from time-lapse time shifts: A geomechanical case study from franklin and elgin f elds, *The Leading Edge*, **26**, 655–662.

Hill, D. P., Reasenberg, P. A., Michael, A., Arabaz, W. J., Beroza, G., Brumbaugh, D., Brune, J. N., Castro, R., Davis, S., dePolo, D., Ellsworth, W. L., Gomberg, J., Harmsen, S., House, L., Jackson, S. M., Johnson, M. J. S., Jones, L., Keller, R., Malone, S., Munguia, L., Nava, S., Pechmann, J. C., Sanford, A., Simpson, R. W., Smith, R. B., Stark, M., Stickney, M., Vidal, A., Walter, S., Wong, V., & Zollweg, J., 1993. Seismicity remotely triggered by the magnitude 7.3 landers california earthquake, *Science*, **260**, 1617–1623.

Hodgson, N., MacBeth, C., Duranti, L., Rickett, J., & Nihei, K., 2007. Inverting for reservoir pressure changes using time-lapse time strain: Application to genesis f eld, gulf of mexico, *The Leading Edge*, **26**, 649–652.

Iyer, H. M. & Hirahara, K., 1993. *Seismic Tomography: Theory and Practice*, Springer-Verlag, New York.

Jaeger, J. C., Cook, N. G. W., & Zimmerman, R. W., 2007. *Fundamentals of Rock Mechanics*, Blackwell Publishing, Oxford.

Jeffrey, A. & Kawahara, T., 1982. *Asymptotic Methods in Nonlinear Wave Theory*, Pitman Advanced Publishing, Boston.

Jeffrey, A. & Taniuti, T., 1964. *Nonlinear Wave Propagation*, Academic Press, New York.

Keller, J. B. & Lewis, R. M., 1995. Asymptotic methods for partial differential equations: The reduced wave equation, and maxwell's equations, in *Surveys in Applied Mathematics*, edited by J. P. Keller, D. W. McLaughlin, & G. C. Papanicolaou, vol. 1, chap. 1, Plenum Press.

Kevorkian, J. & Cole, J. D., 1996. *Multiple Scale and Singular Perturbation Problems*, Springer-Verlag, New York.

Kline, M. & Kay, I. W., 1979. *Electromagnetic Theory and Geometrical Optics*, Robert E. Krieger Publishing, Huntington, NY.

Korsunsky, S., 1997. *Nonlinear Waves in Dispersive and Dissipative Systems with Coupled Fields*, Addison Wesley Longman Ltd., Essex.

Kravtsov, Y. A. & Orlov, Y. I., 1990. *Geometrical Optics of Inhomogeneous Media*, Springer-Verlag.

Kravtsov, Y. A., Forbes, G. W., & Asatryan, A. A., 1999. Theory and applications of complex rays, in *Progress in Optics*, edited by E. Wolf, vol. XXXIX, chap. I, Elsevier.

Landro, M. & Stammeijer, J., 2004. Quantitative estimation of compaction and velocity changes using 4d impedance and traveltime changes, *Geophysics*, **69**, 949–957.

Lewis, R. W. & Ghafouri, H., 1997. A novel f nite element double-porosity model for multiphase f ow through deformable fractured porous media, *Intern. J. Num. Anal. Meth. Geomech.*, **21**, 789–816.

Lewis, R. W. & Sukirman, Y., 1993. Finite element modeling of three-phase f ow in deforming saturated oil reservoirs, *Intern. J. Num. Anal. Meth. Geomech.*, **17**, 577–598.

Lo, W. C., Sposito, G., & Majer, E., 2006. Low-frequency dilatational wave propagation through fully-saturated poroelastic media, *Advances in Water Resources*, **29**, 408–416.

Luneburg, R. K., 1966. *Mathematical Theory of Optics*, University of California Press, Berkeley.

Masson, Y. J., Pride, S. R., & Nihei, K. T., 2006. Finite difference modeling of biot's poroelastic equations at seismic frequencies, *Journal of Geophysical Research*, **111**, 1–13.

Maxwell, S. C., Du, J., & Shemeta, J., 2008. Passive seismic and surface monitoring of geomechanical deformation associated with steam injection, *The Leading Edge*, **27**, 1176–1184.

Menke, W., 1984. *Geophysical Data Analysis: Discrete Inverse Theory*, Academic Press, New York.

Minkoff, S., Stone, C., Bryant, S., Peszynska, M., & Wheeler, M., 2003. Coupled f uid f ow and geomechanical deformation modeling, *Journal of Petroleum Science and Engineering*, **38**, 37–56.

Minkoff, S., Stone, C., Bryant, S., & Peszynska, M., 2004. Coupled geomechanics and f ow simulation for time-lapse seismic modeling, *Geophysics*, **69**, 200–211.

Noble, B. & Daniel, J. W., 1977. *Applied Linear Algebra*, Prentice-Hall, Englewood Cliffs, NJ.

Nolet, G., 1987. *Seismic Tomography*, D. Reidel Publ. Co., Amsterdam.

Noorishad, J., Tsang, C. G., & Witherspoon, P. A., 1984. Coupled thermal-hydraulic-mechanical phenomena in saturated fractures porous rocks: Numerical approach, *Journal of Geophysical Research*, **89**, 10365–10373.

Peaceman, D. W., 1977. *Fundamentals of Numerical Reservoir Simulation*, Elsevier Scientif c Publishing.

Press, W. H., Teukolsky, S. A., Vetterling, W. T., & Flannery, B. P., 1992. *Numerical Recipes*, Cambridge University Press, Cambridge.

Pride, S. R., 2005. Relationships between seismic and hydrological properties, in *Hydrogeophysics*, pp. 253–291, Springer, New York.

Rice, J. R. & Cleary, M. P., 1976. Some basic stress diffusion solutions for f uid-saturated elastic porous media with compressible constituents, *Rev. Geophys. Space. Phys.*, **14**, 227–241.

Rickett, J., Duranti, L., Hudson, T., Regel, B., & Hodgson, N., 2007. 4d time strain and the seismic signatureof geomechanical compaction at genesis, *The Leading Edge*, **26**, 644–647.

Roste, T., Landro, M., & Hatchell, P., 2007. Monitoring overburden layer changes and fault movements from time-lapse seismic data on the valhall f eld, *Geophysical Journal International*, **170**, 1100–1118.

Rudnicki, J. W., 1986. Fluid mass sources and point forces in linear elastic diffusive solids, *Mechanics of Materials*, **5**, 383–393.

Rutqvist, J., Wu, Y. S., Tsang, C. F., & Bodvarsson, G., 2002. A modeling approach for analysis of coupled multiphase f uid f ow, heat transfer, and deformation in fractured porous rock, *Intern. J. of Rock Mech. and Mining Sci.*, **39**, 429–442.

Schutjens, P., Burrell, R., Fehmers, G., Kindriks, K., Collins, C., & van der Horst, J., 2007. On the stress change in overburden resulting from reservoir compation: Observations from two computer models and implications for 4d seismic, *The Leading Edge*, **26**, 628–634.

Segall, P., 1985. Stress and subsidence resulting from subsurface f uid withdrawal in the epicentral region of the 1983 coalinga earthquake, *J. Geophys. Res.*, **90**, 6801–6816.

Sethian, J. A., 1999. *Level Set and Fast Marching Methods*, Cambridge University Press, Cambridge.

Shapiro, S. A., Rothert, E., Rath, V., & Rindschwentner, J., 2002. Characterization of f uid transport properties of reservoirs using induced microseismicity, *Geophysics*, **67**, 212–220.

Showalter, R. E., 2000. Diffusion in poro-elastic media, *J. Math. Anal. Appl.*, **251**, 310–340.

Showalter, R. E. & Stefanelli, U., 2004. Diffusion in poro-plastic media, *Math. Meth. Appl. Sci.*, **27**, 2131–2151.

Simon, B. R., Zienkiewicz, O. C., & Paul, D. K., 1984. An analytical solution for the transient response of saturated porous elastic solids, *Intern. J. Num. Anal. Meth. Geomech.*, **8**, 381–398.

Spiegel, M. R., 1959. *Theory and Problems of Vector Analysis*, McGraw-Hill, New York.

Spiegel, M. R., 1990. *Theory and Problems of Laplace Transforms*, McGraw-Hill, New York.

Stancliffe, R. P. W. & van der Kooij, M. W. A., 2001. The use of satellite-based radar interferometry to monitor production activity at the cold lake heavy oil f eld, alberta canada, *AAPG Bulletin*, **85**, 781–793.

Staples, R., Ita, J., Burrell, R., & Nash, R., 2007. Monitoring pressure depletion and improving geomechanical models of the shearwater f eld using 4d seismic, *The Leading Edge*, **26**, 636–642.

Theis, C., 1935. The relation between the lowering of the piezometric surface and the rate and duration of discharge of a well using groundwater storage, in *Transactions of the AGU*, pp. 519–524, American Geophysical Union, San Francisco.

Thomson, C., 1983. Ray-theoretical amplitude inversion for laterally varying velocity structure below norsar, *Geophys. J. Roy. Astr. Soc.*, **74**, 525–558.

Tura, A., Barker, T., Cattermile, P., Collins, C., Davis, J., Hatchell, P., Koster, K., Schuttjens, P., & Willis, P., 2005. Monitoring primary depletion reservoirs using amplitudes and time-shifts from high-repeat seismic surveys, *The Leading Edge*, **24**, 1214–1221.

Vasco, D., 2004. An asymptotic solution for two-phase f ow in the presence of capillary forces, *Water Resources Research*, **40**, W12407.

Vasco, D., 2007. Trajectory-based modeling of broadband electromagnetic wavef elds, *Geophysical Journal International*, **168**, 949–963.

Vasco, D., 2008a. Modeling quasi-static poroelastic propagation using an asymptotic approach, *Geophysical Journal International*, **173**, 1119–1135.

Vasco, D., 2008b. Zeroth-order inversion of transient pressure observations, *Inverse Problems*, **24**, 1–21.

Vasco, D., 2009. Modeling f ow in a pressure-sensitive, heterogeneous medium, *Geophysical Journal International*, **(in press)**.

Vasco, D., Karasaki, K., & Keers, H., 2000. Estimation of reservoir properties using transient pressure: An asymptotic approach, *Water Resources Research*, **36**, 3447–3465.

Vasco, D., Keers, H., Peterson, J. E., & Majer, E., 2003. Zeroth-order asymptotics: Waveform inversion of the lowest degree, *Geophysics*, **68**, 614–628.

Vasco, D., Ferretti, A., & Novali, F., 2008. Estimating permeability from quasi-static deformation: Temporal variations and arrival-time inversion, *Geophsics*, **73**, O37–O52.

Vidale, J., 1988. Finite-difference calculation of travel times, *Bulletin of the Seismological Society of America*, **78**, 2062–2076.

Virieux, J., Flores-Luna, C., & Gibert, D., 1994. Asymptotic theory for diffusive electromagnetic imaging, *Geophys. J. Int.*, **119**, 857–868.

Wang, H. F., 2000. *Theory of Linear Poroelasticity with Applications to Geomechanics and Hydrogeology*, Princeton Univerisity Press, Princeton, NJ.

Wang, R. & Kumpel, H.-J., 2003. Poroelasticity: Eff cient modeling of strongly coupled, slow deformation processes in a multilayered half-space, *Geophysics*, **68**, 705–717.

Wu, Y. & Pruess, K., 2000. Integral solutions for transient f uid f ow through a porous medium with pressure-dependent permeability, *Int. J. Rock Mech. and Min. Sci.*, **37**, 51–61.

Zimmerman, R. W., 2000. Coupling in poroelasticity and thermoelasticity, *International Journal of Rock Mechanics and Mining Sciences*, **37**, 79–87.

5 APPENDIX A: THE METHOD OF MULTIPLE SCALES

In this Appendix I apply the method of multiple scales (Anile et al., 1993; Kevorkian & Cole, 1996) to the equations governing the evolution of a transient disturbance in a poroelastic medium, equations (15) and (16). These coupled linear partial differential equations depend on the spatially-varying parameters $G(\mathbf{x})$, $K_u(\mathbf{x})$, $C(\mathbf{x})$, $M(\mathbf{x})$, and $K(\mathbf{x})$ as well as on the frequency ω. One approach to solving this system of equations makes use of a series representation of the solution in powers of $1/\omega$ and assumes that ω is large. Because I am interested in modeling disturbances across a wide range of frequencies I shall not adopt this approach. Rather, I will assume that the heterogeneity is smoothly-varying in comparison to scale of the disturbance in displacement and pressure. Specif - cally, if I denote the scale length of the heterogeneity by L and the scale length over which the pressure and displacement varies by l. Then, by assumption, $L \gg l$ and the ratio $\varepsilon = l/L$ is much smaller then 1. In order to bring out the scale separation I can re-write the governing equations in terms of a slow variable $\mathbf{X}$ which is given by

$$\mathbf{X} = \varepsilon \mathbf{x}. \qquad (A1)$$

Furthermore, I can represent the Fourier transform of solid matrix displacement and the pore f uid displacement as power series in ε

$$\mathbf{U}(\mathbf{X},\omega,\theta) = e^{i\theta} \sum_{l=0}^{\infty} \varepsilon^l \mathbf{U}_l(\mathbf{X},\omega) \qquad (A2)$$

$$\mathbf{W}(\mathbf{X},\omega,\theta) = e^{i\theta} \sum_{l=0}^{\infty} \varepsilon^l \mathbf{W}_l(\mathbf{X},\omega). \qquad (A3)$$

Note that, because $\varepsilon \ll 1$, only the f rst few terms of the power series are signif cant. The form of the solutions (A2) and (A3) is a variation of the generalized plane wave expansion used in the study of elastic and electromagnetic waves (Luneburg 1966, Kline and Kay 1979, Aki and Richards 1980, Kravtsov and Orlov 1990) where $\theta(\mathbf{x},\omega)$ is the phase of the disturbance, a quantity related to the propagation time. The phase is a rapidly varying quantity which scales as $1/\varepsilon$ (Anile et al., 1993). After Fourier transforming, the frequency only enters as part of the coeff cients of the governing equations and I shall treat ω as a parameter. The differential operators in the governing equations may be written in terms of the slow variable $\mathbf{X}$ by noting that

$$\frac{\partial \mathbf{U}}{\partial x_i} = \varepsilon \frac{\partial \mathbf{U}}{\partial X_i} + \frac{\partial \theta}{\partial x_i}\frac{\partial \mathbf{U}}{\partial \theta}. \qquad (A4)$$

Hence, making use of equation (A1) I can write the gradient operators as

$$\nabla \mathbf{U} = \varepsilon \nabla_{\mathbf{X}} \mathbf{U} + \nabla\theta \frac{\partial \mathbf{U}}{\partial \theta} \qquad (A5)$$

$$\nabla \cdot \mathbf{U} = \varepsilon \nabla_{\mathbf{X}} \cdot \mathbf{U} + \nabla\theta \cdot \frac{\partial \mathbf{U}}{\partial \theta} \qquad (A6)$$

where $\nabla_{\mathbf{X}}$ denotes the gradient with respect to the components of the slow variable $\mathbf{X}$. In the derivation that follows I shall suppress the $\mathbf{X}$ subscript on the differential operator ∇.

The f rst step involves re-writing the governing equations in terms of the slow variables. Consider a version of the f rst equation (15) in which I expand the derivative terms

$$\begin{aligned}
&\nabla G \cdot \nabla \mathbf{U} \\
&+\nabla G \cdot (\nabla \mathbf{U})^T \\
&-\frac{2}{3}\nabla G \cdot [(\nabla \cdot \mathbf{U})\,\mathbf{I}] \\
&+G\nabla \cdot \nabla \mathbf{U} \\
&+G\nabla \cdot (\nabla \mathbf{U})^T \\
&-\frac{2}{3}G\nabla \cdot [(\nabla \cdot \mathbf{U})\,\mathbf{I}] \\
&+\nabla K_u \nabla \cdot \mathbf{U} \\
&+K_u \nabla (\nabla \cdot \mathbf{U}) \\
&+\nabla C \nabla \cdot \mathbf{W} \\
&+C\nabla (\nabla \cdot \mathbf{W}) \\
&+\omega^2 \rho \mathbf{U} + \omega^2 \rho_f \mathbf{W} = 0. \qquad (A7)
\end{aligned}$$

Now I substitute the differential operators as indicated in (A5) and (A6), only retaining terms containing $\varepsilon^0 \sim 1$ and ε^1,

$$\begin{aligned}
&\varepsilon \nabla G \cdot \left(\nabla\theta \frac{\partial \mathbf{U}}{\partial \theta}\right) \\
&+\varepsilon \nabla G \cdot \left(\nabla\theta \frac{\partial \mathbf{U}}{\partial \theta}\right)^T \\
&-\varepsilon \frac{2}{3}\nabla G \cdot \left[\left(\nabla\theta \cdot \frac{\partial \mathbf{U}}{\partial \theta}\right)\mathbf{I}\right] \\
&+\varepsilon G\nabla \cdot \left(\nabla\theta \frac{\partial \mathbf{U}}{\partial \theta}\right) + \varepsilon G\nabla\theta \cdot \nabla\left(\frac{\partial \mathbf{U}}{\partial \theta}\right) + G\nabla\theta \cdot \left(\nabla\theta \frac{\partial^2 \mathbf{U}}{\partial \theta^2}\right) \\
&+\varepsilon G\nabla \cdot \left(\nabla\theta \frac{\partial \mathbf{U}}{\partial \theta}\right)^T + \varepsilon G\nabla\theta \cdot \nabla\left(\frac{\partial \mathbf{U}}{\partial \theta}\right)^T + G\nabla\theta \cdot \left(\nabla\theta \frac{\partial^2 \mathbf{U}}{\partial \theta^2}\right)^T \\
&-\varepsilon \frac{2}{3}G\nabla \cdot \left(\nabla\theta \cdot \frac{\partial \mathbf{U}}{\partial \theta}\right)\mathbf{I} - \varepsilon \frac{2}{3}G\nabla\theta \cdot \left(\nabla \cdot \frac{\partial \mathbf{U}}{\partial \theta}\right)\mathbf{I} - \frac{2}{3}G\nabla\theta \cdot \left(\nabla\theta \cdot \frac{\partial^2 \mathbf{U}}{\partial \theta^2}\right)\mathbf{I} \\
&+\varepsilon \nabla K_u \left(\nabla\theta \cdot \frac{\partial \mathbf{U}}{\partial \theta}\right) \\
&+\varepsilon K_u \nabla \left(\nabla\theta \cdot \frac{\partial \mathbf{U}}{\partial \theta}\right) + \varepsilon K_u \nabla\theta \left(\nabla \cdot \frac{\partial \mathbf{U}}{\partial \theta}\right) + K_u \nabla\theta \left(\nabla\theta \cdot \frac{\partial^2 \mathbf{U}}{\partial \theta^2}\right) \\
&+\varepsilon \nabla C \left(\nabla\theta \cdot \frac{\partial \mathbf{W}}{\partial \theta}\right) \\
&+\varepsilon C \nabla \left(\nabla\theta \cdot \frac{\partial \mathbf{W}}{\partial \theta}\right) + \varepsilon C \nabla\theta \left(\nabla \cdot \frac{\partial \mathbf{W}}{\partial \theta}\right) + C\nabla\theta \left(\nabla\theta \cdot \frac{\partial^2 \mathbf{W}}{\partial \theta^2}\right) \\
&+\omega^2 \rho \mathbf{U} + \omega^2 \rho_f \mathbf{W} = 0. \qquad (A8)
\end{aligned}$$

I can write equation (A8) more compactly if I use the def nition of $\mathbf{p} = \nabla\theta$ and the fact that

$$\frac{\partial \mathbf{U}}{\partial \theta} = i\mathbf{U}$$

and

$$\frac{\partial \mathbf{W}}{\partial \theta} = i\mathbf{W}$$

which follows from the form of the solutions (A2) and (A3). Making these substitutions, I can write equation (A8) as

$$\varepsilon \nabla G \cdot (i\mathbf{p}\mathbf{U})$$

$$+\varepsilon \nabla G \cdot (i\mathbf{p}\mathbf{U})^T$$

$$-\varepsilon \frac{2}{3} \nabla G \cdot [(i\mathbf{p} \cdot \mathbf{U})\, \mathbf{I}]$$

$$+\varepsilon G \nabla \cdot (i\mathbf{p}\mathbf{U}) + \varepsilon G \mathbf{p} \cdot \nabla (i\mathbf{U}) - G\mathbf{p} \cdot (\mathbf{p}\mathbf{U})$$

$$+\varepsilon G \nabla \cdot (i\mathbf{p}\mathbf{U})^T + \varepsilon G \mathbf{p} \cdot (\nabla i\mathbf{U})^T - G\mathbf{p} \cdot (\mathbf{p}\mathbf{U})^T$$

$$-\varepsilon \frac{2}{3} G \nabla \cdot (i\mathbf{p} \cdot \mathbf{U})\, \mathbf{I} - \varepsilon \frac{2}{3} G \mathbf{p} \cdot (\nabla \cdot i\mathbf{U})\, \mathbf{I} + \frac{2}{3} G \mathbf{p} \cdot (\mathbf{p} \cdot \mathbf{U})\, \mathbf{I}$$

$$+\varepsilon \nabla K_u (i\mathbf{p} \cdot \mathbf{U})$$

$$+\varepsilon K_u \nabla (i\mathbf{p} \cdot \mathbf{U}) + \varepsilon K_u \mathbf{p} (\nabla \cdot i\mathbf{U}) - K_u \mathbf{p} (\mathbf{p} \cdot \mathbf{U})$$

$$+\varepsilon \nabla C (i\mathbf{p} \cdot \mathbf{W})$$

$$+\varepsilon C \nabla (i\mathbf{p} \cdot \mathbf{W}) + \varepsilon C \mathbf{p} (\nabla \cdot i\mathbf{W}) - C\mathbf{p} (\mathbf{p} \cdot \mathbf{W})$$

$$+\omega^2 \rho \mathbf{U} + \omega^2 \rho_f \mathbf{W} = 0. \qquad (A9)$$

Some of the terms in equation (A9) can be expanded to arrive at

$$i\varepsilon \mathbf{p} (\nabla G \cdot \mathbf{U})$$

$$+i\varepsilon (\nabla G \cdot \mathbf{p})\, \mathbf{U}$$

$$-i\varepsilon \frac{2}{3} \nabla G (\mathbf{p} \cdot \mathbf{U})$$

$$+i\varepsilon G [(\nabla \cdot \mathbf{p})\, \mathbf{U} + 2\mathbf{p} \cdot (\nabla \mathbf{U})] - G\mathbf{p} (\mathbf{p} \cdot \mathbf{U})$$

$$+i\varepsilon G \left[(\nabla \cdot \mathbf{U})\mathbf{p} + \mathbf{U} \cdot \nabla \mathbf{p} + \mathbf{p} \cdot (\nabla \mathbf{U})^T\right] - Gp^2 \mathbf{U}$$

$$-i\varepsilon \frac{2}{3} G [\nabla (\mathbf{p} \cdot \mathbf{U}) + (\nabla \cdot \mathbf{U})\, \mathbf{p}] + \frac{2}{3} G \mathbf{p} (\mathbf{p} \cdot \mathbf{U})$$

$$+i\varepsilon \nabla K_u (\mathbf{p} \cdot \mathbf{U})$$

$$+i\varepsilon K_u [\nabla (\mathbf{p} \cdot \mathbf{U}) + \mathbf{p} (\nabla \cdot \mathbf{U})] - K_u \mathbf{p} (\mathbf{p} \cdot \mathbf{U})$$

$$+i\varepsilon \nabla C (\mathbf{p} \cdot \mathbf{W})$$

$$+i\varepsilon C [\nabla (\mathbf{p} \cdot \mathbf{W}) + \mathbf{p} (\nabla \cdot \mathbf{W})] - C\mathbf{p} (\mathbf{p} \cdot \mathbf{W})$$

$$+\omega^2 \rho \mathbf{U} + \omega^2 \rho_f \mathbf{W} = 0. \qquad (A10)$$

Considering the second governing equation (16), expanding the derivatives I arrive at

$$\nabla C \nabla \cdot \mathbf{U}$$

$$C \nabla \nabla \cdot \mathbf{U}$$

$$\nabla M \nabla \cdot \mathbf{W}$$

$$+M \nabla \nabla \cdot \mathbf{W}$$

$$\omega^2 \rho_f \mathbf{U} + \omega^2 \tilde{\rho} \mathbf{W} = 0. \qquad (A11)$$

Substituting the differential operators and retaining terms of order ε^0 and ε^1,

$$\varepsilon \nabla C \left(\nabla \theta \cdot \frac{\partial \mathbf{U}}{\partial \theta}\right)$$

$$+\varepsilon C \nabla \left(\nabla \theta \cdot \frac{\partial \mathbf{U}}{\partial \theta}\right) + \varepsilon C \nabla \theta \left(\nabla \cdot \frac{\partial \mathbf{U}}{\partial \theta}\right) + C \nabla \theta \left(\nabla \theta \cdot \frac{\partial^2 \mathbf{U}}{\partial \theta^2}\right)$$

$$\varepsilon \nabla M \left(\nabla \theta \cdot \frac{\partial \mathbf{W}}{\partial \theta}\right)$$

$$+\varepsilon M \nabla \left(\nabla \theta \cdot \frac{\partial \mathbf{W}}{\partial \theta}\right) + \varepsilon M \nabla \theta \left(\nabla \cdot \frac{\partial \mathbf{W}}{\partial \theta}\right) + M \nabla \theta \left(\nabla \theta \cdot \frac{\partial^2 \mathbf{W}}{\partial \theta^2}\right)$$

$$\omega^2 \rho_f \mathbf{U} + \omega^2 \tilde{\rho} \mathbf{W} = 0. \qquad (A12)$$

Using the def nition of $\mathbf{p}$ and the property of the partial derivatives I can write equation (A12) as

$$i\varepsilon \nabla C (\mathbf{p} \cdot \mathbf{U})$$

$$+i\varepsilon C [\nabla (\mathbf{p} \cdot \mathbf{U}) + \mathbf{p} (\nabla \cdot \mathbf{U})] - C\mathbf{p} (\mathbf{p} \cdot \mathbf{U})$$

$$i\varepsilon \nabla M (\mathbf{p} \cdot \mathbf{W})$$

$$+i\varepsilon M [\nabla (\mathbf{p} \cdot \mathbf{W}) + \mathbf{p} (\nabla \cdot \mathbf{W})] - M\mathbf{p} (\mathbf{p} \cdot \mathbf{W})$$

$$\omega^2 \rho_f \mathbf{U} + \omega^2 \tilde{\rho} \mathbf{W} = 0. \qquad (A13)$$

5.1 Terms of Order $\varepsilon^0 \sim 1$

As noted above, because ε is assumed to be small, the terms of lowest order are the most signif cant. To f nd these terms I substitute the power series expressions for $\mathbf{U}$ and $\mathbf{W}$, given by (A2) and (A3), into equations (A10) and (A12). Two equations result, each containing an inf nite progression of terms of various orders in ε. If I consider terms of the lowest order in ε, $\varepsilon^0 \sim 1$, I arrive at the two equations

$$Gp^2 \mathbf{U}_0 + \frac{1}{3} G \mathbf{p}\mathbf{p} \cdot \mathbf{U}_0 + K_u \mathbf{p}\mathbf{p} \cdot \mathbf{U}_0 - \omega^2 \rho \mathbf{U}_0$$

$$+C\mathbf{p}\mathbf{p} \cdot \mathbf{W}_0 - \omega^2 \rho_f \mathbf{W}_0 = 0 \qquad (A14)$$

and

$$C\mathbf{p}\mathbf{p} \cdot \mathbf{U}_0 - \omega^2 \rho_f \mathbf{U}_0 + M\mathbf{p}\mathbf{p} \cdot \mathbf{W}_0 - \omega^2 \tilde{\rho} \mathbf{W}_0 = 0. \quad (A15)$$

5.2 Terms of Order ε^1

Now consider terms of the next lowest order in ε, those of f rst order. For the f rst equation (A10), I have

$$i\mathbf{p} (\nabla G \cdot \mathbf{U}_0)$$

$$+i (\nabla G \cdot \mathbf{p})\, \mathbf{U}_0$$

$$-i\frac{2}{3}\nabla G\left(\mathbf{p}\cdot\mathbf{U}_0\right)$$

$$+iG\left[\left(\nabla\cdot\mathbf{p}\right)\mathbf{U}_0+2\mathbf{p}\cdot\left(\nabla\mathbf{U}_0\right)\right]-G\mathbf{p}\left(\mathbf{p}\cdot\mathbf{U}_1\right)$$

$$+iG\left[\left(\nabla\cdot\mathbf{U}_0\right)\mathbf{p}+\mathbf{U}_0\cdot\nabla\mathbf{p}+\mathbf{p}\cdot\left(\nabla\mathbf{U}_0\right)^T\right]-Gp^2\mathbf{U}_1$$

$$-i\frac{2}{3}G\left[\nabla\left(\mathbf{p}\cdot\mathbf{U}_0\right)+\left(\nabla\cdot\mathbf{U}_0\right)\mathbf{p}\right]+\frac{2}{3}G\mathbf{p}\left(\mathbf{p}\cdot\mathbf{U}_1\right)$$

$$+i\nabla K_u\left(\mathbf{p}\cdot\mathbf{U}_0\right)$$

$$+iK_u\left[\nabla\left(\mathbf{p}\cdot\mathbf{U}_0\right)+\mathbf{p}\left(\nabla\cdot\mathbf{U}_0\right)\right]-K_u\mathbf{p}\left(\mathbf{p}\cdot\mathbf{U}_1\right)$$

$$+i\nabla C\left(\mathbf{p}\cdot\mathbf{W}_0\right)$$

$$+iC\left[\nabla\left(\mathbf{p}\cdot\mathbf{W}_0\right)+\mathbf{p}\left(\nabla\cdot\mathbf{W}_0\right)\right]-C\mathbf{p}\left(\mathbf{p}\cdot\mathbf{W}_1\right)$$

$$+\omega^2\rho\mathbf{U}_1+\omega^2\rho_f\mathbf{W}_1=0 \qquad (A16)$$

where I have substituted in the first two terms $\mathbf{U}_0$, $\mathbf{U}_1$, $\mathbf{W}_0$, and $\mathbf{W}_1$ of the power series (A2) and (A3). Similarly, for equation (A13) I have

$$i\nabla C\left(\mathbf{p}\cdot\mathbf{U}_0\right)$$

$$+iC\left[\nabla\left(\mathbf{p}\cdot\mathbf{U}_0\right)+\mathbf{p}\left(\nabla\cdot\mathbf{U}_0\right)\right]-C\mathbf{p}\left(\mathbf{p}\cdot\mathbf{U}_1\right)$$

$$i\nabla M\left(\mathbf{p}\cdot\mathbf{W}_0\right)$$

$$+iM\left[\nabla\left(\mathbf{p}\cdot\mathbf{W}_0\right)+\mathbf{p}\left(\nabla\cdot\mathbf{W}_0\right)\right]-M\mathbf{p}\left(\mathbf{p}\cdot\mathbf{W}_1\right)$$

$$\omega^2\rho_f\mathbf{U}_1+\omega^2\tilde{\rho}\mathbf{W}_1=0. \qquad (A17)$$

6 APPENDIX B: DIFFERENTIAL EQUATIONS FOR U_0 AND W_0

In this Appendix I discuss how to transform the coupled system of linear, first-order differential equations (82) into two uncoupled second-order equations. First, consider two equations in (82)

$$\frac{dU_0}{dr}=-\Gamma_{11}U_0-\Gamma_{12}W_0 \qquad (B1)$$

$$\frac{dW_0}{dr}=-\Gamma_{21}U_0-\Gamma_{22}W_0. \qquad (B2)$$

I can solve equation (B1) for W_0 in terms of U_0 and its derivative

$$W_0=-\frac{1}{\Gamma_{12}}\left[\frac{dU_0}{dr}+\Gamma_{11}U_0\right]. \qquad (B3)$$

Substituting this expression into equation (B2) for W_0, carrying out the differentiations, and grouping terms gives

$$\frac{1}{\Gamma_{12}}\frac{d^2U_0}{dr^2}+\left[\frac{d}{dr}\left(\frac{1}{\Gamma_{12}}\right)+\frac{\Gamma_{11}}{\Gamma_{12}}+\frac{\Gamma_{22}}{\Gamma_{12}}\right]\frac{dU_0}{dr}$$

$$+\left[\frac{d}{dr}\left(\frac{\Gamma_{11}}{\Gamma_{12}}-\Gamma_{21}+\frac{\Gamma_{11}\Gamma_{22}}{\Gamma_{12}}\right)\right]U_0=0. \qquad (B4)$$

Multiplying equation (B4) by Γ_{12} and defining the coefficients

$$\Psi_1(r)=\Gamma_{12}\frac{d}{dr}\left(\frac{1}{\Gamma_{12}}\right)+\Gamma_{11}+\Gamma_{22} \qquad (B5)$$

$$\Psi_2(r)=\Gamma_{12}\frac{d}{dr}\left(\frac{\Gamma_{11}}{\Gamma_{12}}\right)-\Gamma_{12}\Gamma_{21}+\Gamma_{11}\Gamma_{22} \qquad (B6)$$

I can write equation (B4) as

$$\frac{d^2U_0}{dr^2}+\Psi_1\frac{dU_0}{dr}+\Psi_2U_0=0, \qquad (B7)$$

a second-order differential equation for U_0 with variable coefficients. Following a similar procedure I can derive a governing equation for W_0

$$\frac{d^2W_0}{dr^2}+\Phi_1\frac{dW_0}{dr}+\Phi_2W_0=0, \qquad (B8)$$

where

$$\Phi_1(r)=\Gamma_{21}\frac{d}{dr}\left(\frac{1}{\Gamma_{21}}\right)+\Gamma_{11}+\Gamma_{22} \qquad (B9)$$

$$\Phi_2(r)=\Gamma_{21}\frac{d}{dr}\left(\frac{\Gamma_{22}}{\Gamma_{21}}\right)-\Gamma_{12}\Gamma_{21}+\Gamma_{11}\Gamma_{22}. \qquad (B10)$$

Rather than solving equation (B7) and (B8) it might be more efficient to solve equation (B7) for U_0 and then use equation (B3) to find W_0.

Figure 1. Source function used to generate the pressure pulse for the numerical finite-difference modeling. It was also used in the convolution with the point source response to generate the analytic and asymptotic solutions.

Figure 2. Three snapshots from the finite-difference modeling of Biot's poroelastic equations. The snapshots display the pressure variation due to the source pulse, shown in Figure 1, applied at the center of the simulation grid. The observation point, the location at which the time variation of pressure is calculated, is indicated by an open triangle.

Figure 3. A comparison of the numerical calculation of pressure (Numeric), an analytic solution for pressure (Analytic), and the asymptotic solution (Asymptotic) given by equation (125). Each pressure curve has been normalized such that its peak value is unity.

Figure 4. The difference between the asymptotic solution and the numeric and analytic solutions. The error is given in terms of the percentage of the normalized peak value. Thus, in this case, the error never exceeds roughly 2 percent of the peak value.

Figure 5. Three snapshots from the finite-difference modeling of Biot's poroelastic equations. The snapshots show the radial displacement of the solid matrix due to the pressure pulse shown in Figure 1.

Figure 6. A comparison of the numerical calculation of the radial displacement of the solid matrix, an analytic solution for the displacement, and the asymptotic solution given by equation (146). Each curve has been normalized the peak value of displacement.

Figure 7. The difference between the asymptotic solution and the numeric and analytic solutions. The differences are given in terms of their percentage of the peak value of the displacement curves, in this case 1.

Figure 8. The velocity variation of the Biot slow wave for the calculation of pressure and displacement in a heterogeneous medium. The model contains a high velocity layer bounded above and below by low velocity zones. The velocity of the layer also increases linearly to the right.

Figure 9. A snapshot of the pressure 1000s after the beginning of injection into the heterogeneous model. The source time function, given in Figure 1, is identical to that used in the modeling for the homogeneous medium.

Figure 10. The variation of phase associated with the Biot slow wave, due to the heterogeneous velocity structure. The phase was calculated by numerically solving the eikonal equation for the velocity variation shown in Figure 8 (Vidale 1988, Sethian 1999). The star denotes the location of the source and the open triangle denotes the location of the observation point. The trajectory which represents the propagation path of the slow wave is indicated by the solid curve.

Figure 11. A comparison of the numerical calculation of pressure and the asymptotic solution given by equation (125). Both pressure curves have been normalized such that their peak values are unity.

Figure 12. The difference between the asymptotic solution and the numeric solution. The error is given in terms of the percentage of the normalized peak value.

Figure 13. A comparison of the numerical calculation of the radial displacement of the solid matrix and the asymptotic solution given by equation (146). Each curve has been normalized the peak value of displacement.

Figure 14. The difference between the asymptotic solution for radial displacement and the numeric solution.

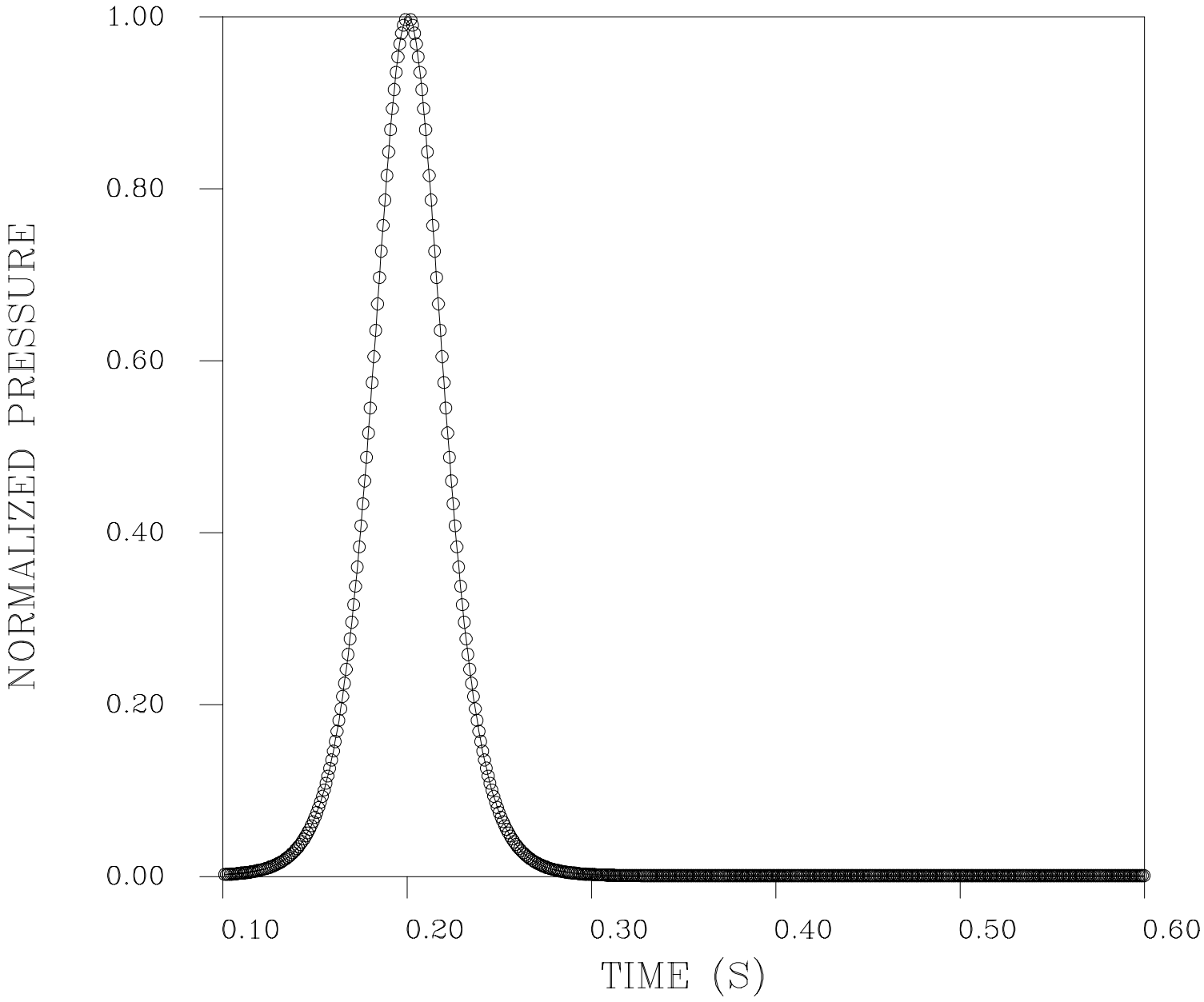
1.00
0.80
0.60
0.40
0.20
0.00
NORMALIZED PRESSURE
0.10
0.20
0.30
0.40
0.50
0.60
TIME (S)

Figure 1.

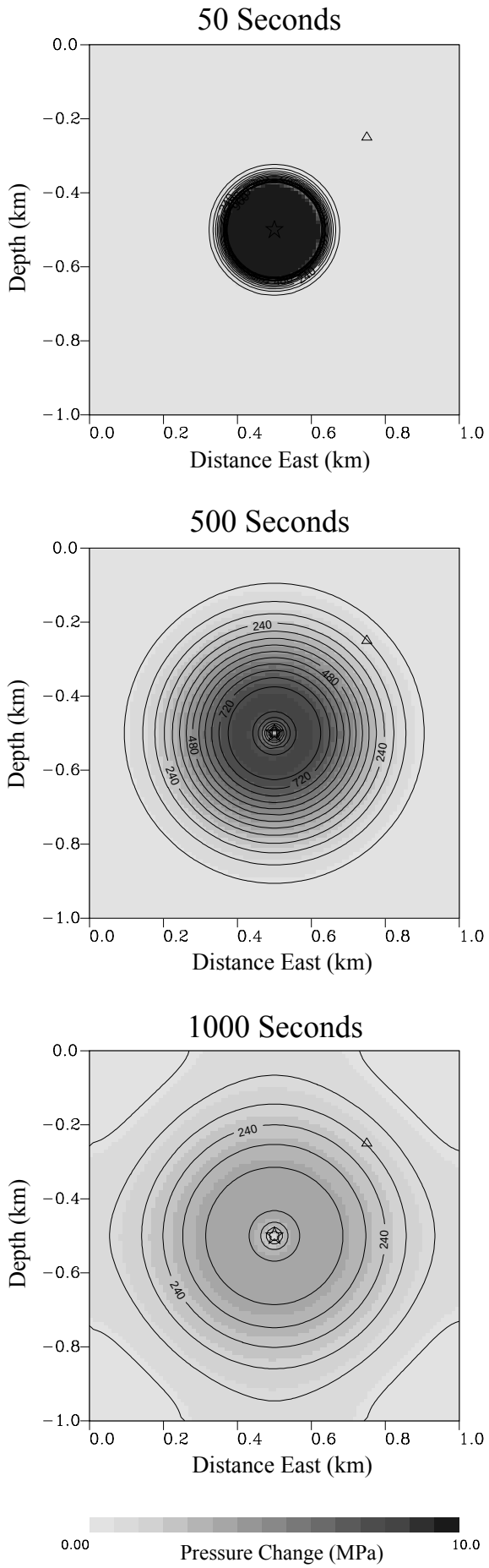
50 Seconds
500 Seconds
1000 Seconds
Depth (km)
Distance East (km)
0.0
−0.2
−0.4
−0.6
−0.8
−1.0
0.2
0.4
0.6
0.8
1.0
240
480
720
0.00
10.0
Pressure Change (MPa)

Figure 2.

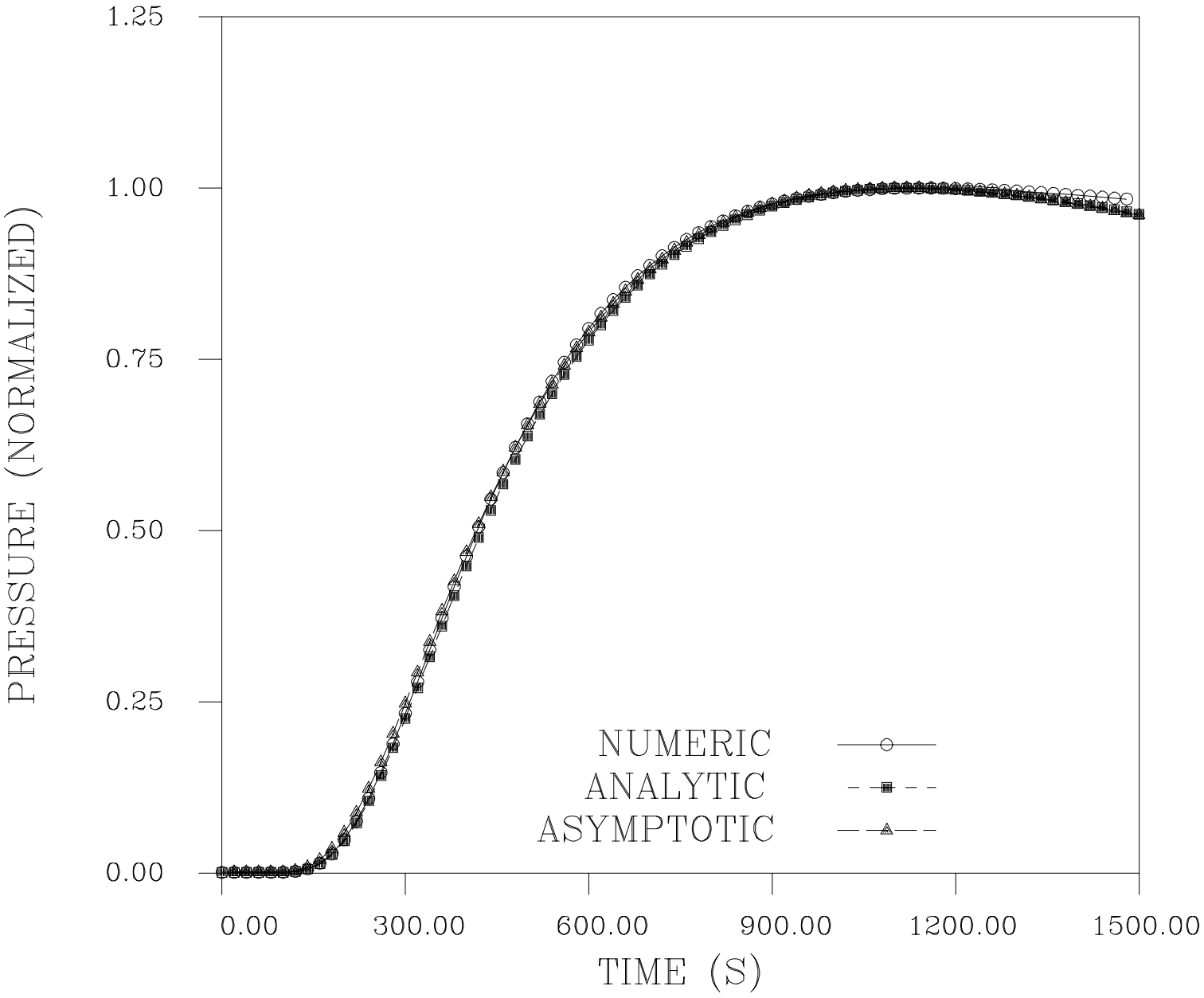
1.25
1.00
0.75
0.50
0.25
0.00
PRESSURE (NORMALIZED)
0.00
300.00
600.00
900.00
1200.00
1500.00
TIME (S)
NUMERIC
ANALYTIC
ASYMPTOTIC

Figure 3.

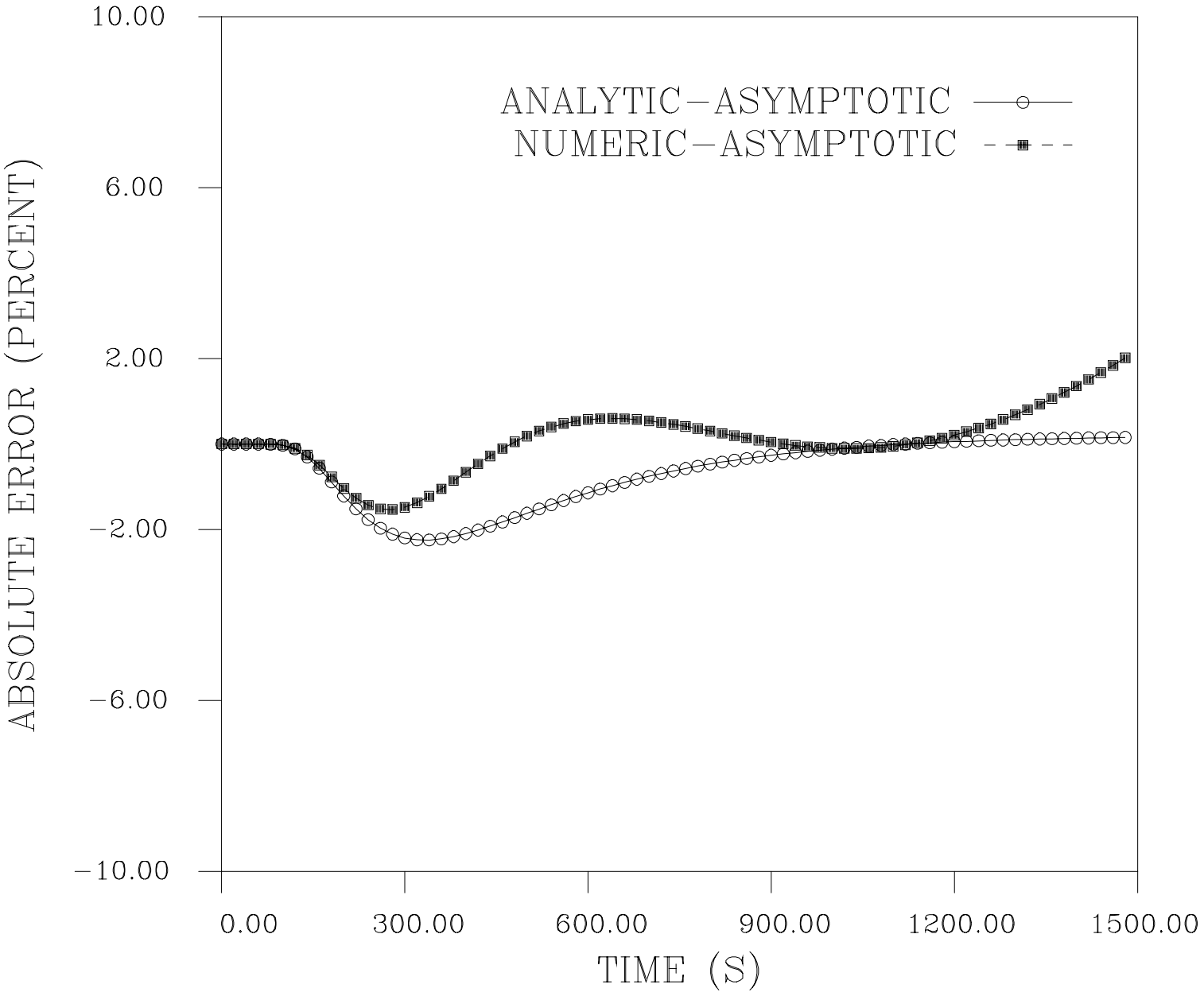
ANALYTIC−ASYMPTOTIC
NUMERIC−ASYMPTOTIC
ABSOLUTE ERROR (PERCENT)
10.00
6.00
2.00
−2.00
−6.00
−10.00
0.00
300.00
600.00
900.00
1200.00
1500.00
TIME (S)

Figure 4.

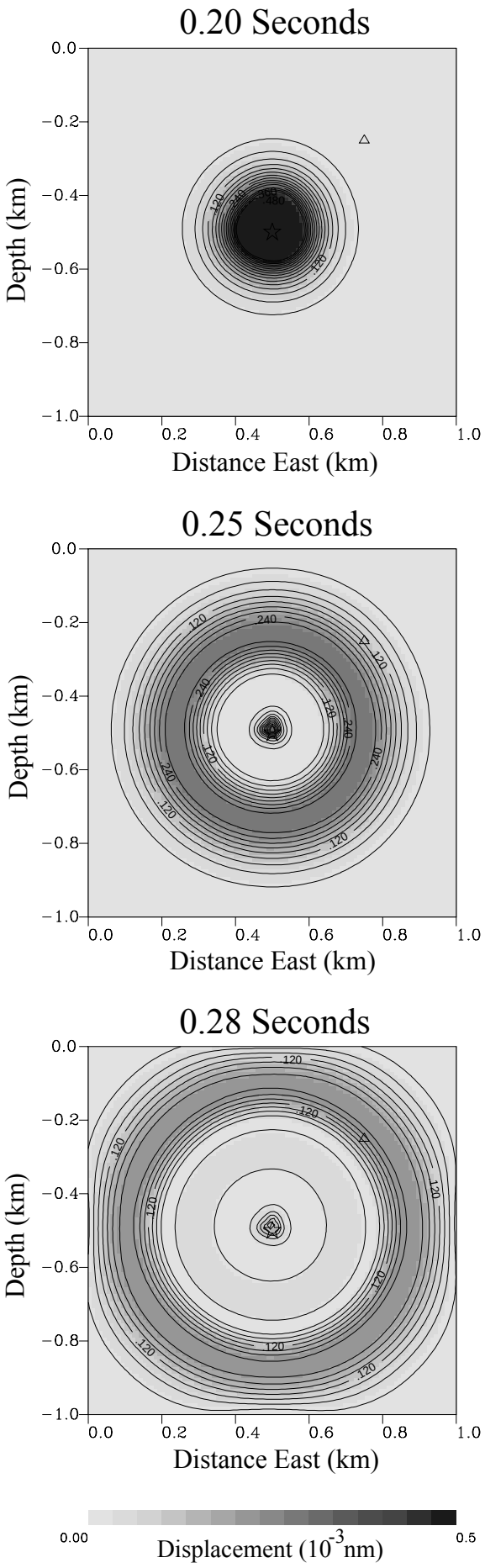
0.20 Seconds
0.25 Seconds
0.28 Seconds
Depth (km)
Distance East (km)
0.0
−0.2
−0.4
−0.6
−0.8
−1.0
0.2
0.4
0.6
0.8
1.0
120
240
360
480
0.00
0.5
Displacement (10^{-3}nm)

Figure 5.

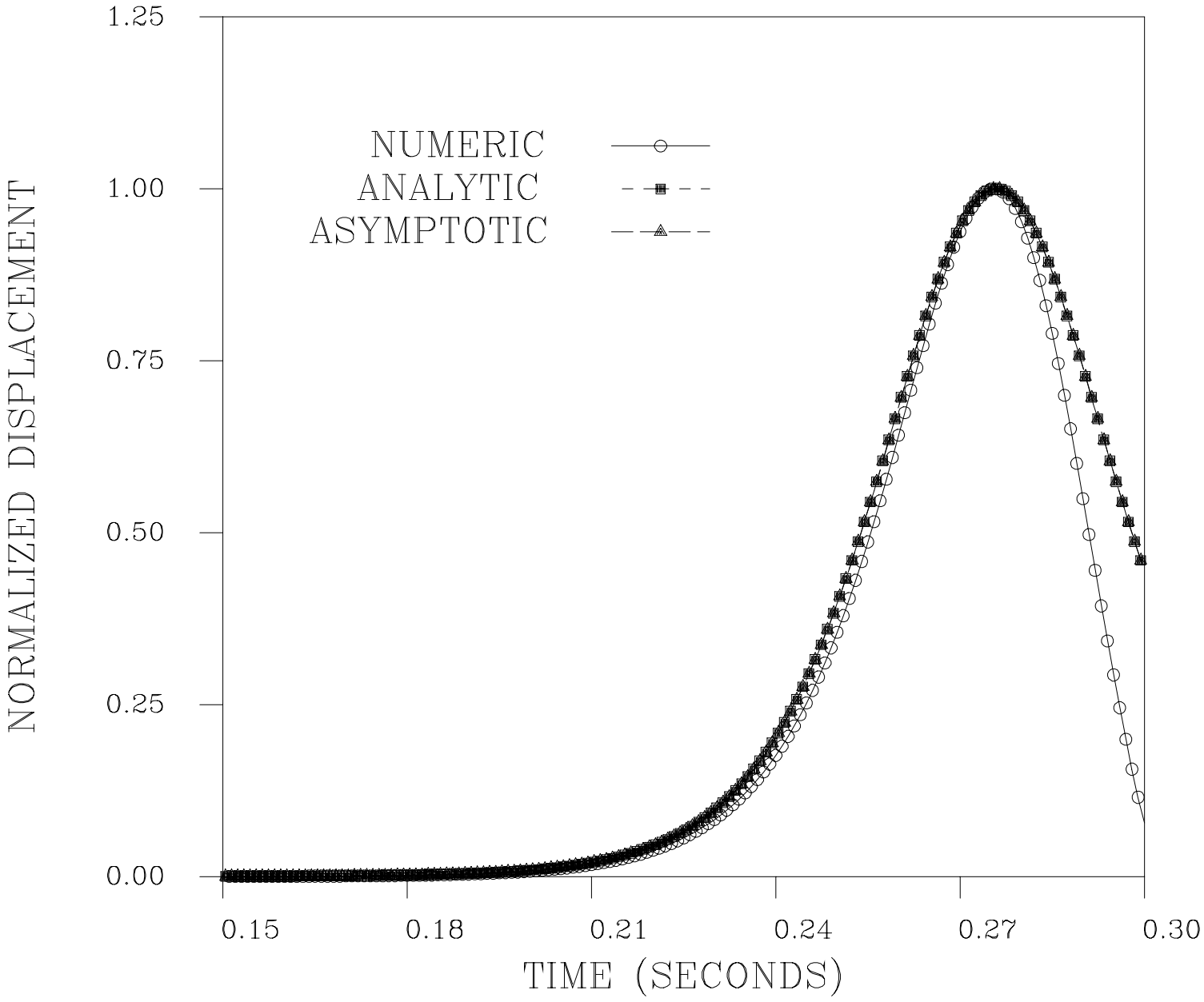
NUMERIC
ANALYTIC
ASYMPTOTIC
NORMALIZED DISPLACEMENT
1.25
1.00
0.75
0.50
0.25
0.00
0.15
0.18
0.21
0.24
0.27
0.30
TIME (SECONDS)

Figure 6.

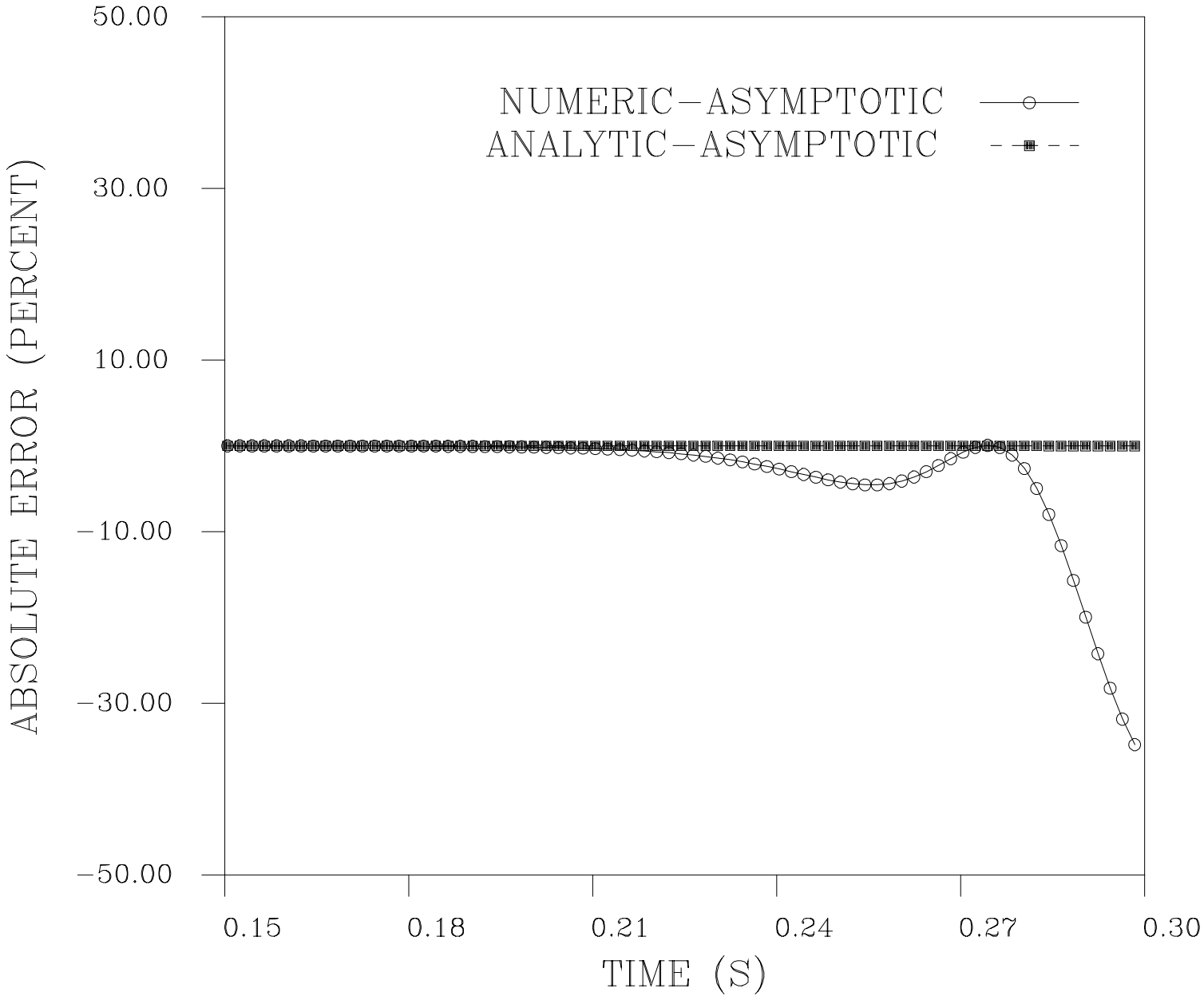
50.00
30.00
10.00
−10.00
−30.00
−50.00
ABSOLUTE ERROR (PERCENT)
NUMERIC−ASYMPTOTIC
ANALYTIC−ASYMPTOTIC
0.15
0.18
0.21
0.24
0.27
0.30
TIME (S)

Figure 7.

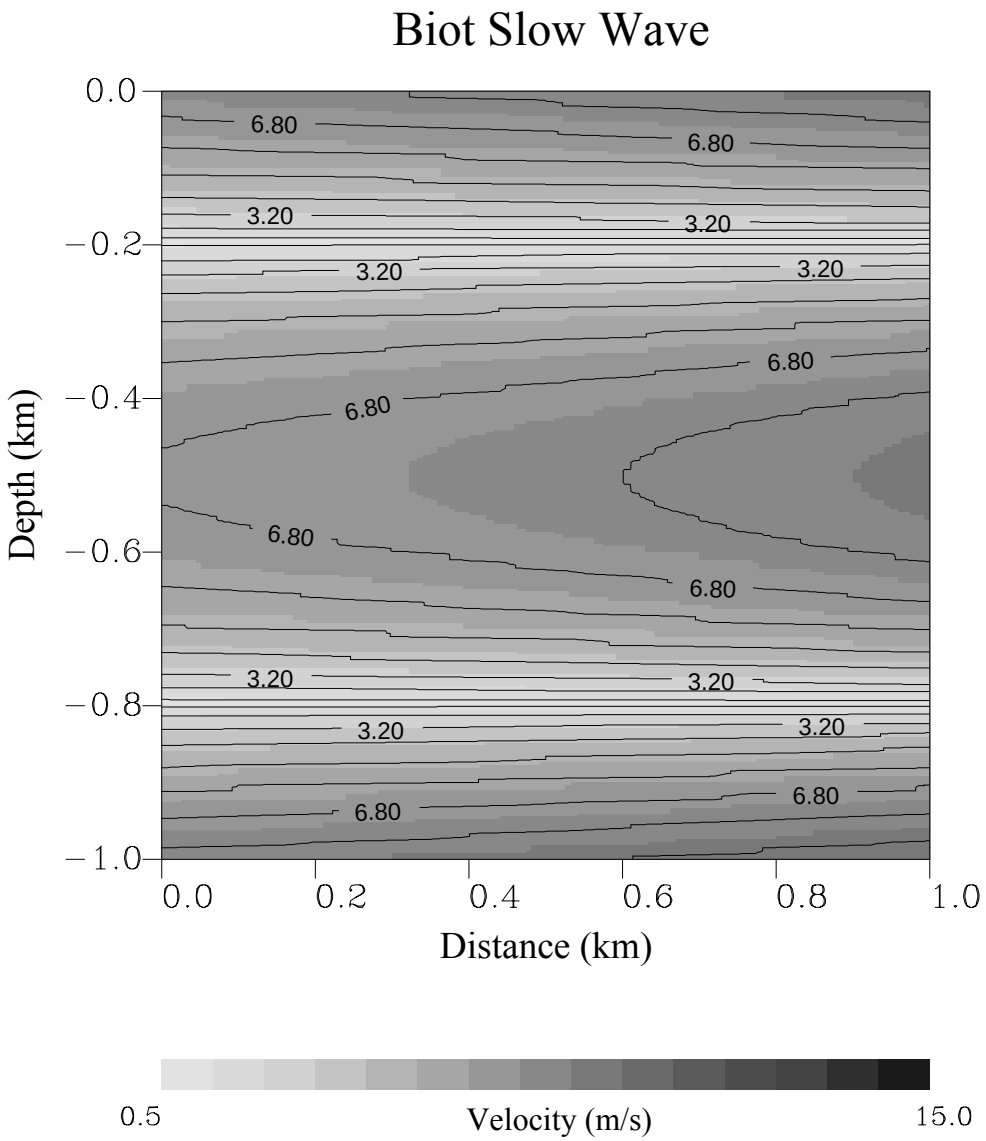
Biot Slow Wave
0.0
−0.2
−0.4
−0.6
−0.8
−1.0
Depth (km)
6.80
3.20
0.0
0.2
0.4
0.6
0.8
1.0
Distance (km)
0.5
Velocity (m/s)
15.0
CONTOUR FROM 0.50000 TO 14.900 CONTOUR INTERVAL OF 0.90000 PT(3,3)= 7.7270

Figure 8.

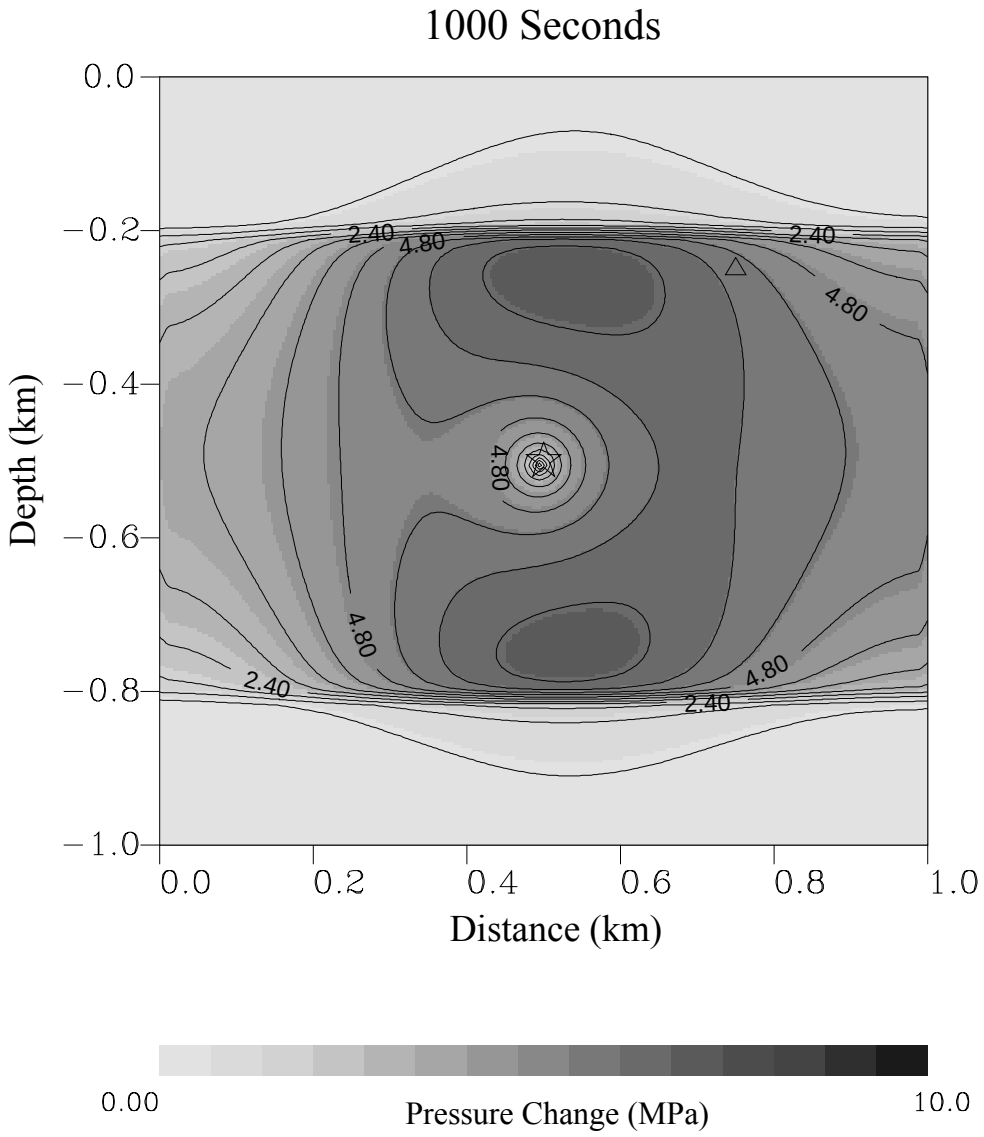
1000 Seconds
0.0
−0.2
−0.4
−0.6
−0.8
−1.0
Depth (km)
2.40
4.80
2.40
4.80
4.80
4.80
2.40
4.80
2.40
0.0
0.2
0.4
0.6
0.8
1.0
Distance (km)
0.00
Pressure Change (MPa)
10.0
CONTOUR FROM 0. TO 9.6000 CONTOUR INTERVAL OF 0.60000 PT(3,3)= 0.63972E-01

Figure 9.

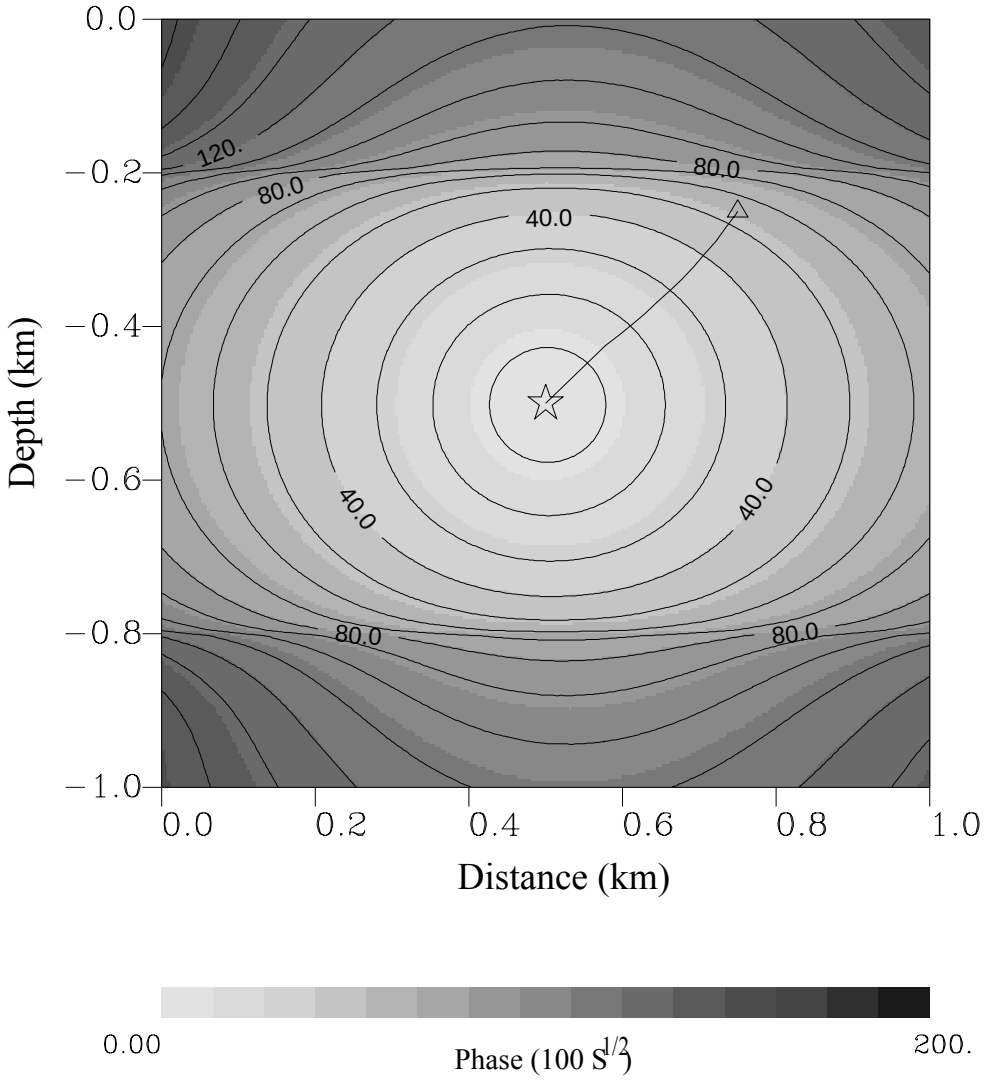

CONTOUR FROM 0. TO 200.00 CONTOUR INTERVAL OF 10.000 PT(3,3)= 146.64

Figure 10.

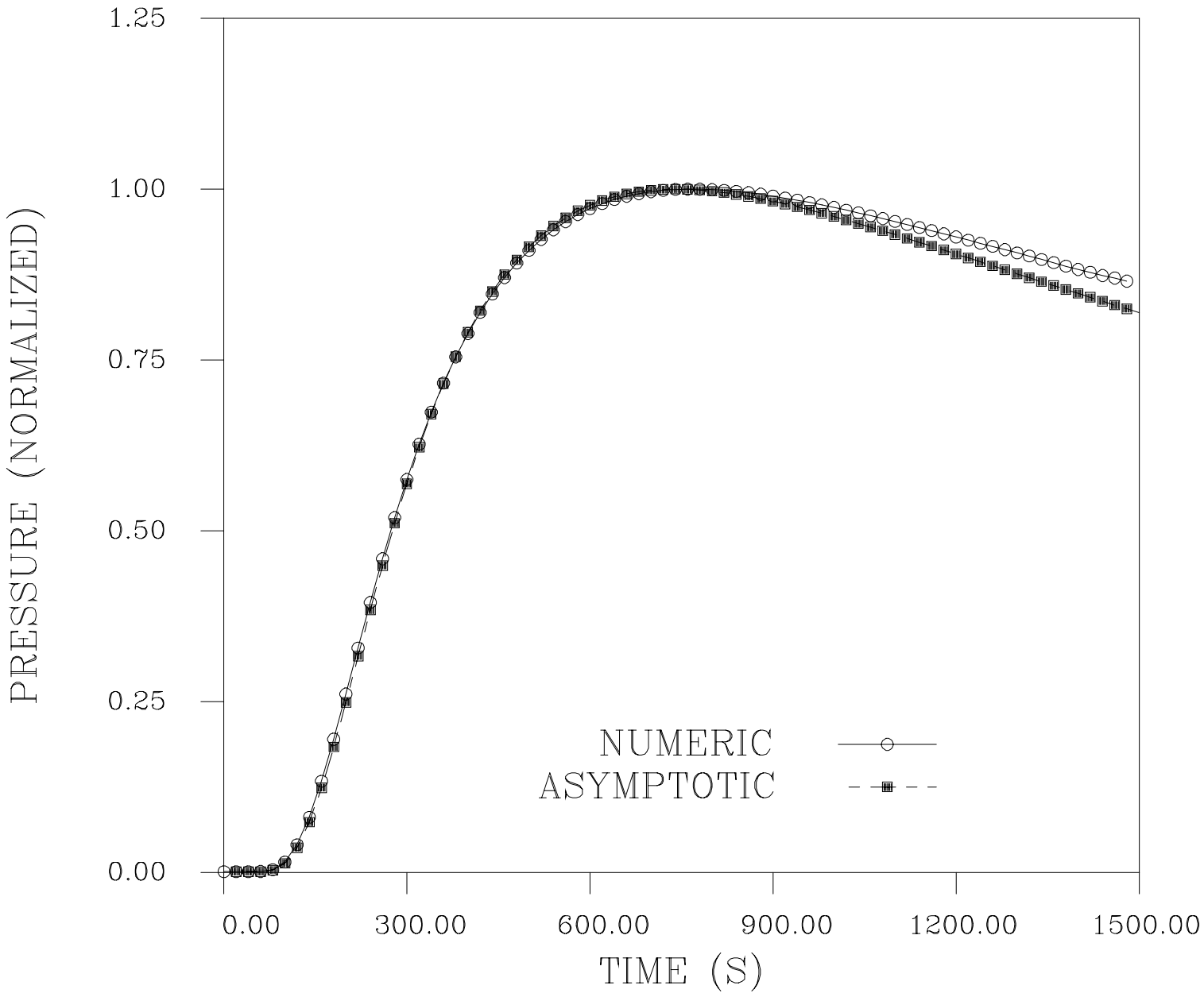
1.25
1.00
0.75
0.50
0.25
0.00
PRESSURE (NORMALIZED)
0.00
300.00
600.00
900.00
1200.00
1500.00
TIME (S)
NUMERIC
ASYMPTOTIC

Figure 11.

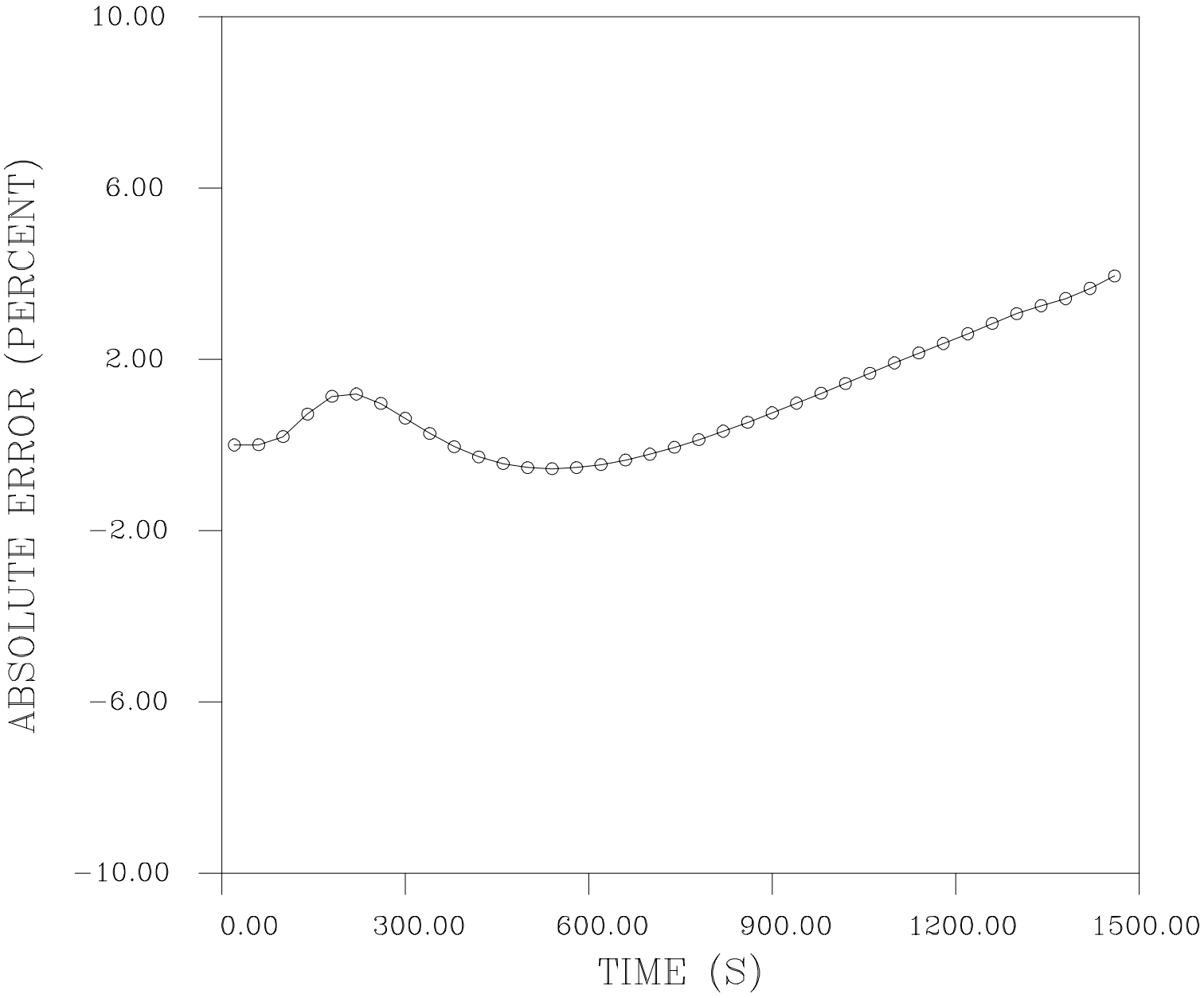
10.00
6.00
2.00
−2.00
−6.00
−10.00
ABSOLUTE ERROR (PERCENT)
0.00
300.00
600.00
900.00
1200.00
1500.00
TIME (S)

Figure 12.

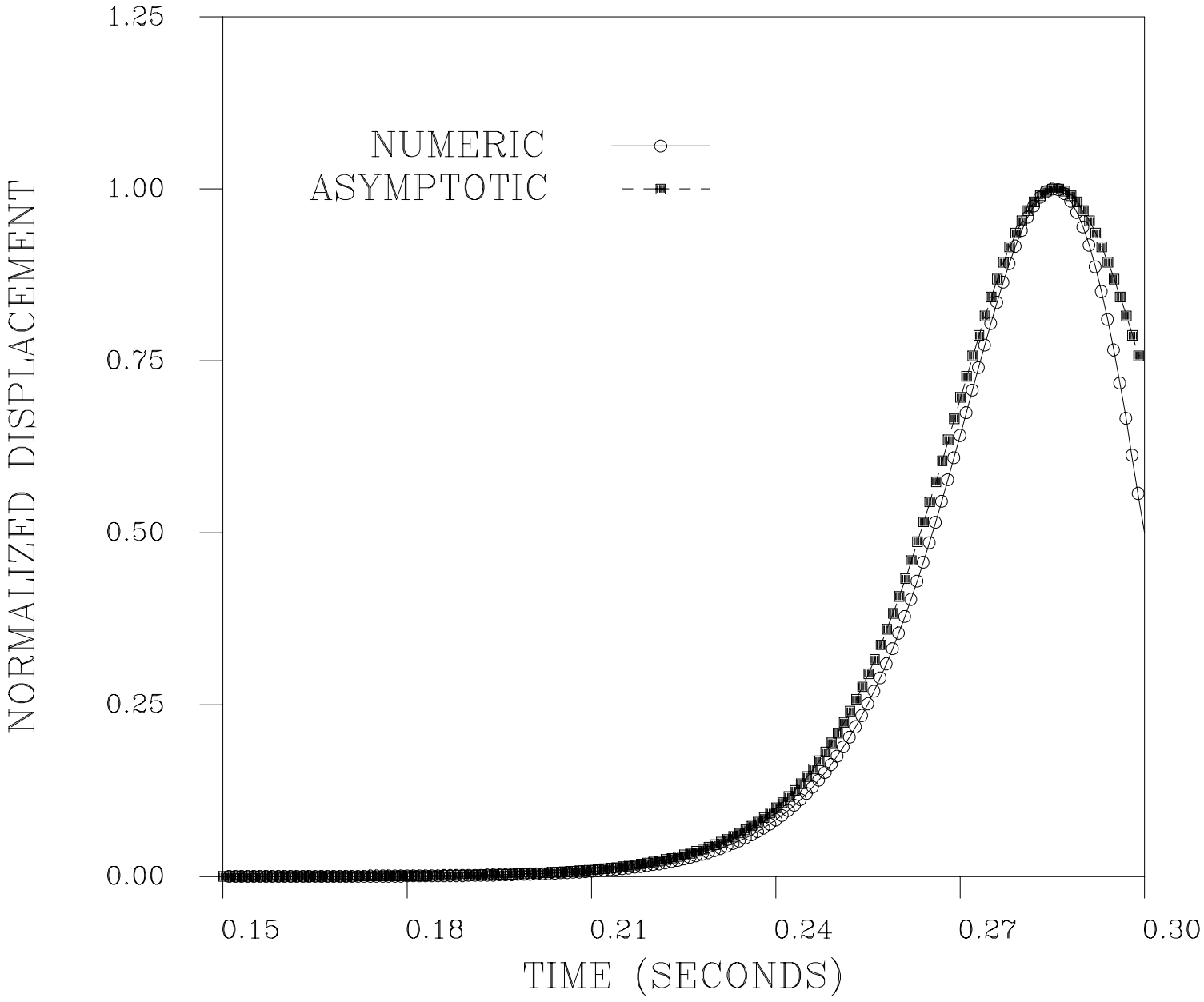
NUMERIC
ASYMPTOTIC
NORMALIZED DISPLACEMENT
1.25
1.00
0.75
0.50
0.25
0.00
0.15
0.18
0.21
0.24
0.27
0.30
TIME (SECONDS)

Figure 13.

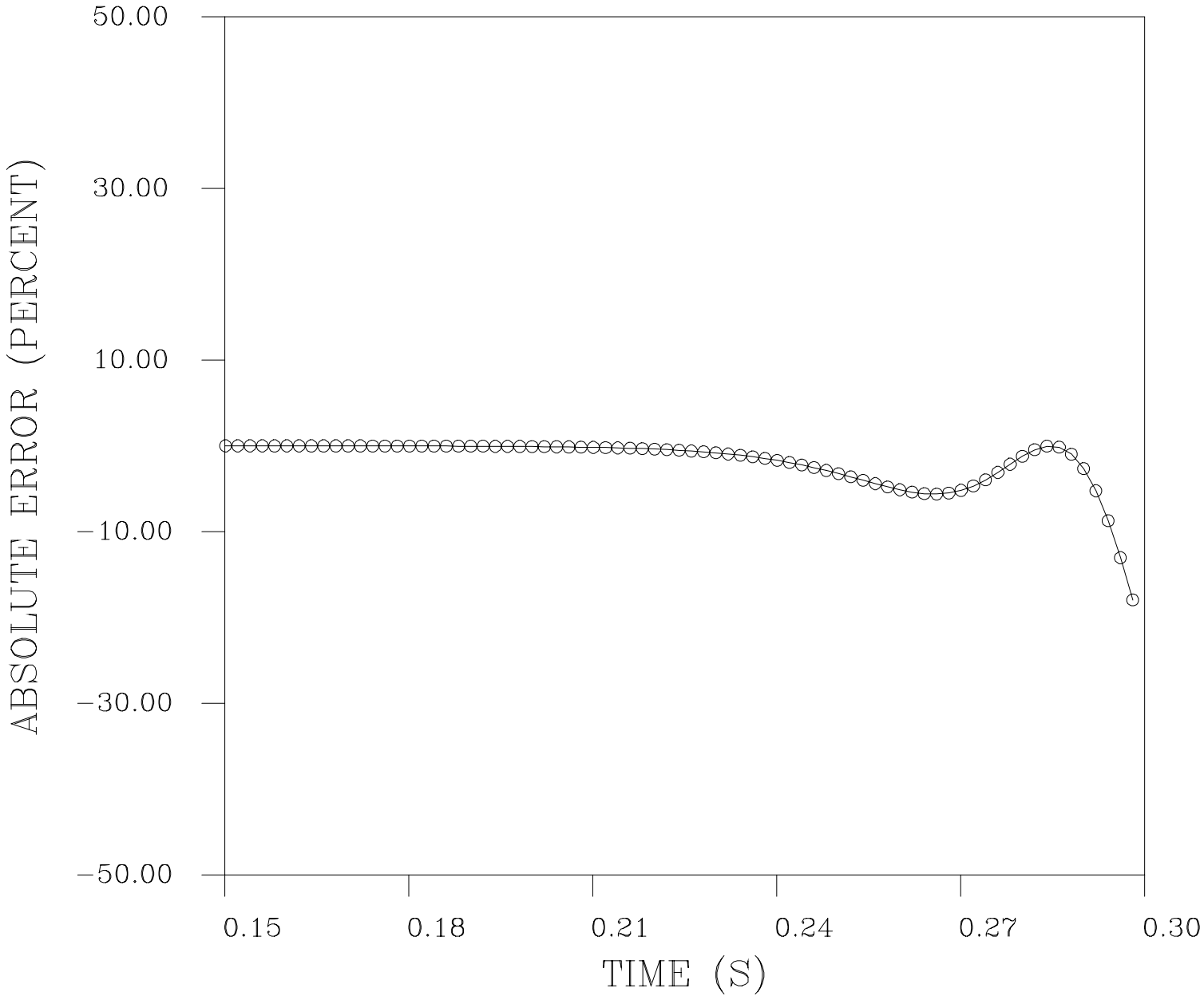
50.00
30.00
10.00
−10.00
−30.00
−50.00
ABSOLUTE ERROR (PERCENT)
0.15
0.18
0.21
0.24
0.27
0.30
TIME (S)

Figure 14.